CoCliCo

Research and Innovation Action (RIA)

This project has received funding from the European Union's Horizon 2020 research and innovation programme under grant agreement No 101003598

Start date : 2021-09-01 Duration : 48 Months

Vulnerability metrics for Europe

Authors : Dr. Elco KOKS (VU Amsterdam), Joël De Plaen (IVM-VU), Sadhana Nirandjan (IVM-VU), Tristian Stolte (IVM-VU), Vincent Bascoul (BRGM), Philip Ward (IVM-VU)

CoCliCo - Contract Number: 101003598

Project officer: Anna Natasa ASIK

Document title	Vulnerability metrics for Europe
Author(s)	Dr. Elco KOKS, Joël De Plaen (IVM-VU), Sadhana Nirandjan (IVM-VU), Tristian Stolte (IVM-VU), Vincent Bascoul (BRGM), Philip Ward (IVM-VU)
Number of pages	56
Document type	Deliverable
Work Package	WP5
Document number	D5.3
Issued by	VU Amsterdam
Date of completion	2024-05-28 10:25:27
Dissemination level	Public

Summary

Europe?s coastal communities are vulnerable to coastal flooding. This vulnerability, exacerbated by Europe?s aging infrastructure and diverse populations living in coastal areas, necessitates a comprehensive understanding of vulnerability drivers of coastal communities. Vulnerability assessments, crucial components of climate services, provide insights into the pathways from hazard to impact, aiding in informed decision-making for adaptation strategies. Our report focuses on vulnerability curves and indicators, commonly utilized methods in assessing vulnerability, aiming to provide a nuanced understanding of vulnerability to coastal flooding in Europe. Deliverable 5.3 presents a thorough analysis of vulnerability assessment methodologies, synthesizing academic and grey literature to identify and define vulnerability drivers. Through a structured review, we compiled a harmonized database containing fragility and vulnerability curves, laying the groundwork for well-informed risk assessments. Additionally, our efforts led to the operationalization of 206 drivers of coastal flood vulnerability, facilitating the development of a pan-European vulnerability index. While acknowledging the inherent limitations of vulnerability assessments, our report serves as a valuable resource for policymakers, researchers, and practitioners engaged in coastal climate risk management. Looking forward, the insights gained from this deliverable provide a solid foundation for future research and policy interventions aimed at enhancing the resilience of coastal communities and that of critical infrastructure systems in particular. By addressing data gaps, refining methodologies, and integrating local-scale knowledge, stakeholders can better anticipate and mitigate the impacts of climate extremes on critical infrastructure, fostering a more resilient and sustainable future for European coastal societies.

Approval

Date	By
2024-05-28 10:26:08	Dr. Elco KOKS (VU Amsterdam)
2024-05-29 10:15:04	Dr. Gonéri LE COZANNET (BRGM)

D5.3 Coastal flooding vulnerability metrics for Europe

Release Status: FINAL

Dissemination level: Public

Author: Elco Koks (IVM-VU), Joël De Plaen (IVM-VU), Sadhana Nirandjan (IVM-VU), Tristian Stolte (IVM-VU), Vincent Bascoul (BRGM), Philip Ward (IVM-VU)

Date: 24/05/2024

Filename and version: D5.3 CoCliCo.pdf

Project ID NUMBER 101003598

Call: H2020-LC-CLA-2020-2

DG/Agency: CINEA

This project has received funding from the European Union's Horizon 2020 research and innovation programme under grant agreement No. 101003598

Authorisation

This document requires the following approvals:

Authorisation	Name	Signature	Date
Project Coordinator	Goneri Le Cozannet	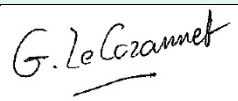	28/05/24
WP Leader	Elco Koks		24/05/24

Disclaimer
The information and views set out in this report are those of the author(s) and do not necessarily reflect the official opinion of the European Union. Neither the European Union institutions and bodies nor any person acting on their behalf may be held responsible for the use which may be made of the information contained therein.

This project has received funding from the European Union's Horizon 2020 research and innovation programme under grant agreement No. 101003598

Executive summary

Europe's coastal communities are vulnerable to coastal flooding. This vulnerability, exacerbated by Europe's aging infrastructure and diverse populations living in coastal areas, necessitates a comprehensive understanding of vulnerability drivers of coastal communities. Vulnerability assessments, crucial components of climate services, provide insights into the pathways from hazard to impact, aiding in informed decision-making for adaptation strategies. Our report focuses on vulnerability curves and indicators, commonly utilized methods in assessing vulnerability, aiming to provide a nuanced understanding of vulnerability to coastal flooding in Europe.

Deliverable 5.3 presents a thorough analysis of vulnerability assessment methodologies, synthesizing academic and grey literature to identify and define vulnerability drivers. Through a structured review, we compiled a harmonized database containing fragility and vulnerability curves, laying the groundwork for well-informed risk assessments. Additionally, our efforts led to the operationalization of 206 drivers of coastal flood vulnerability, facilitating the development of a pan-European vulnerability index. While acknowledging the inherent limitations of vulnerability assessments, our report serves as a valuable resource for policymakers, researchers, and practitioners engaged in coastal climate risk management.

Looking forward, the insights gained from this deliverable provide a solid foundation for future research and policy interventions aimed at enhancing the resilience of coastal communities and that of critical infrastructure systems in particular. By addressing data gaps, refining methodologies, and integrating local-scale knowledge, stakeholders can better anticipate and mitigate the impacts of climate extremes on critical infrastructure, fostering a more resilient and sustainable future for European coastal societies.

This project has received funding from the European Union's Horizon 2020 research and innovation programme under grant agreement No. 101003598

Table of Contents

This project has received funding from the European Union's Horizon 2020 research and innovation programme under grant agreement No. 101003598

1. Introduction

As highlighted in the most recent European Climate Risk Assessment, coastal communities and critical infrastructure in Europe are already at threat to climate extremes, and coastal flooding in particular. This is not only due to sea-level rise, and the increasing frequency and intensity of climate extremes, but also due to aging and deteriorating CI assets and systems (EUCRA, 2024). Vousdoukas et al. (2020) highlight that Europe's exposed population could increase from 100,000 citizens per year to up to 1.6 million a year under a more optimistic climate scenario. Moreover, Christodoulou et al. (2019) and Forzieri et al. (2018), emphasize the vulnerability of port facilities and critical infrastructure networks to coastal flooding in Europe and the escalating impacts on these assets towards the future. To develop sound and robust adaptation strategies, a good understanding of the vulnerability drivers behind these impacts is essential.

The outcome of a disaster is often described by its damage (e.g., Stolte et al., 2023; van Ginkel et al., 2021). The level of damage is determined by the total value of the exposed people and assets (max damage) as well as their vulnerability. Vulnerability is defined by the UNDRR as "the conditions determined by physical, social, economic and environmental factors or processes which increase the susceptibility of an individual, a community, assets or systems to the impacts of hazards" (OIEWG, 2016). Spatiotemporal variations in vulnerability causes differences in the impact between and within societies (e.g. Meijer et al., 2023; Cutter et al., 2003). It is therefore important to account for vulnerability in disaster risk assessments, either quantitatively or qualitatively.

Generally, a distinction is made between physical and social vulnerability (de Ruiter et al., 2017). Physical vulnerability relates to the characteristics of physical objects, like buildings, (critical) infrastructures and vegetation (De Ruiter et al., 2017; Stolte et al., 2024). It is often quantified with vulnerability curves, also called depth-damage curves or intensity-damage curves, which link the intensity of a hazard (i.e. depth of flooding for coastal floods) to the damage caused by that hazard (Meyer et al., 2013). Social vulnerability is about the often-non-visible characteristics of the exposed people, like age, socioeconomic status and access to healthcare. It is often assessed with the help of vulnerability indicators and indexes, which score several vulnerability characteristics to provide an estimate of the overall social vulnerability level (e.g., Meijer et al., 2023; Tapia et al., 2017; Cutter et al., 2003). Although there are other, less-frequently-used, forms of vulnerability assessments like vulnerability matrices (Menoni et al., 2012) or system dynamics models (Joakim et al., 2016), we will focus here on vulnerability curves and indicators/indexes as the most-commonly-applied methods.

Vulnerability assessments are an indispensable part of climate services which have a goal of informing its users about risk and improving their decision making on adaptation (Gerlak and Greene, 2019), as in CoCliCo. These assessments inform the climate-service user about the pathways from hazard to impact and the physical and social characteristics that determine the level of impact. Since climate services are demand-driven tools, users should be allowed to incorporate local-scale knowledge into the service (Findlater et al., 2021). The applicability of vulnerability in a climate service therefore depends on how well it can represent the local vulnerability situation in the region of interest. On the other side, we also want the service to be broadly – European wide – applicable. This tension between broad or deep information is

This project has received funding from the European Union's Horizon 2020 research and innovation programme under grant agreement No. 101003598

a common one in climate-service development (Buontempo et al., 2018). Vulnerability curves and indicators serve well for transferable climate services and could also provide sufficient local-scale context when they are evidence based.

The remainder of this report will provide an extensive overview of (a) fragility and vulnerability curves, based on a systematic literature review of grey (i.e., reports) and academic literature (chapter 2), and (b) vulnerability indicators, based on a comprehensive review of vulnerability drivers, linked to available supranational (urban) datasets (chapter 3). The presented fragility and vulnerability curves provide the basis for the coastal flood risk assessment as performed in CoCliCo's Work Package 6. The collection of vulnerability indicators will allow us to generate a pan-European (social) vulnerability index that can be used to identify the most vulnerable communities along the European coastline, which may not always be necessarily represented by the monetary outcomes of standard natural hazard risk assessments.

This project has received funding from the European Union's Horizon 2020 research and innovation programme under grant agreement No. 101003598

2. Physical vulnerability curves

2.1. Physical vulnerability database for critical infrastructure

The level of physical vulnerability of critical infrastructure to natural hazards plays a pivotal role in understanding, evaluating, and minimizing risks arising from such hazards affecting our critical infrastructure. A common approach to account for the vulnerability of assets in risk assessments that estimate the potential direct damage is by using fragility and vulnerability curves. Vulnerability curves relate given levels of a hazard intensity measure to the potential physical damage of an asset, either in absolute values (e.g., 0 – 165 euros) or in relative numbers (e.g., 0 – 100% damage). These curves are widely used within the flood community for their risk assessments, whereby the flood inundation level is commonly used as the hazard intensity measure; these curves are therefore also known as depth-damage or stage-damage curves. Fragility curves, however, define the relationship between the probability of exceeding a particular damage state (or performance state) of an asset and a hazard intensity measure. A damage state (e.g., slight, complete) describes the level of damage to an element in a qualitative and descriptive way. For example, a power plant may enter the 'extensive' damage state if there is considerable damage observed to motor-driven pumps.

While the vulnerability is a key determinant of risk, researchers encounter challenges that impede the selection and utilization of available fragility and vulnerability curves for critical infrastructure. Firstly, vulnerability information is distributed across literature (e.g., scientific articles, user and technical manuals) instead of being accessible in a centralized dataset. Secondly, curves are not readily available for analysis as often only visualizations are presented. Thirdly, curves are too often presented in an incomplete way. For example, missing functions or parameters to reconstruct the presented curve, or even missing axes when visualizations are presented. The United Nations' Sendai Framework for Disaster Risk Reduction emphasizes the necessity for efforts to mitigate vulnerabilities and advocates for the promotion of freely available and accessible vulnerability information to facilitate effective risk management (UNDRR, 2015)

Recently, a harmonized freely accessible database that contains fragility and vulnerability curves for critical infrastructure has been developed to advance the disaster risk community to perform risk assessments that are supported by well-informed decisions based on the status-quo of vulnerability literature. Nirandjan et al. (2024) conducted a systematic literature review of both academic and grey literature to derive an overview of available infrastructure fragility and vulnerability curves for a selection of hazard types, namely, flooding, earthquakes, windstorms, and landslides. The publicly available database contains over 1,510 curves that can directly be used as input for risk assessment studies. Besides the collection of the curves, Nirandjan et al. (2024) also collected hazard (e.g., intensity measure), exposure (e.g., detailed description of asset), and vulnerability characteristics for each curve (e.g., derivation methodology) to aid the understanding of the underlying assumptions, which may help users to better evaluate the reliability, accuracy, and overall quality of the curves. Moreover, the database also contains cost estimates for critical infrastructure retrieved from the reviewed literature. These cost values can be used in combination with the curves for risk studies focussing on direct physical damages to infrastructure. In the remainder of this chapter, we specifically discuss the flood curves and the associated cost estimates that are available within

This project has received funding from the European Union's Horizon 2020 research and innovation programme under grant agreement No. 101003598

the database, which is accessible via the following Zenodo repository: https://zenodo.org/doi/10.5281/zenodo.10203845.

2.2. Coverage across critical infrastructure types

The database presents 117 unique flood curves for seven overarching critical infrastructure systems: energy, transportation, telecommunication water, waste, health, and education. The coverage of these curves across critical infrastructure systems varies widely. More than half of the database comprises curves for the transportation system (31.3%) and water system (25.3%), while only a limited number of curves exist for the telecommunication system (2.2%).

In the current body of literature, predominantly vulnerability curves are available for which generally expert judgement and/or empirical data is used for the development of the (often more generalized) curves. Conversely, analytical approaches with a strong focus on object-based physical attributes of an asset are commonly applied for the development of fragility curves. Additionally, it is worth noting that flood inundation is used as the hazard intensity measure for 87% of the curves, while other hazard intensities such as flow velocity remain understudied despite of their significant contribution to flood damage. Furthermore, the vulnerability curves are predominantly retrieved from technical reports for flood risk modelling, especially from those for the Netherlands and for the United States (US). Specifically for the US, the Federal Emergency Management Agency (FEMA) developed extensive technical manuals to assess hazard risks from flooding, earthquakes, tsunamis and hurricanes. The 2013 flood manual (FEMA, 2013) contributes with 46.5% to the total number of curves within the database.

We briefly explain the fragility and vulnerability curves as well as the cost estimates (reference year of 2020) that are compiled by Nirandjan et al. (2024) in the following sections per critical infrastructure system. We also present visualizations of these curves. Please note that the curves can be identified by the unique identifier numbers (e.g., F1.1), which are used to specifically refer to curves throughout the systematic review of Nirandjan et al. (2024) as well as in the publicly available database.

2.2.1. Energy

Vulnerability curves for plants and substations were developed by FEMA (2013), thereby considering a range of construction designs considering the capacity of energy generation. They categorize small, medium and large power plants, which are characterized by a power generation of <100 MW, 100-500 MW, and >500 MW (FEMA, 2021). For the development of the damage functions, the depth of flooding within a power plant is compared to the height of critical components within the given power plant. Here, the general assumption is that electrical switch gear is located at a height of 0.91 m above ground level. Specifically for small power plants, they also assume that support facilities are damaged on ground level, and that control and generation facilities are damaged when flood water depths are reaching higher levels. The curve for the damage functions for the three categories of power plants are identical. For substations, they include substations with a of functionality transmission (138-765 kV) and sub-transmission (34.5-161 kV, which are further categorized as small (low voltage: 34.5-150 kV), medium (medium voltage: 150-350 kV), and large (high voltage: >350 kV) substations. Here, the general assumption is that electrical switch gear is located at a height of 0.91 m above ground level, damage to the control room starts at the onset of the flood and is maximized

This project has received funding from the European Union's Horizon 2020 research and innovation programme under grant agreement No. 101003598

when reaching a water level of 2.13 m, and that electrical components (e.g. cabling, transformers, and switchgear) are damaged as well. Similar to the power plant curves, vulnerability curves for the three categories of substations are identical. For risk assessments the vulnerability functions are used in combination with replacement costs which ranges between 194-974 million euros and 11-55 million euros for power plants and substations, respectively, depending on the capacity.

Furthermore, Miyamoto International (MI, 2019) presents generalized vulnerability curves for a wide range of infrastructure types for application at the global scale, which are predominantly based on adaptation of curves presented in existing literature such as FEMA (2013) using expert judgement. They assume that wind turbines globally are not vulnerable to flooding. Also, Vanneuville et al. (2006), and Meyer and Messner (2005) developed vulnerability curves for wind farms in Belgium and Germany, respectively. The former presents a maximum damage value of 705,000 euros. MI (2019) also provides an expert-judgement based curve for coal, gas, or oil-based thermal plants. FEMA (2013) provides curves for the transmission and distribution circuit (T&D). A generalized curve for the energy system within the Netherlands is provided by Kok et al. (2005) based on a limited amount of damage data and expert judgement. No curves were found for power towers and poles. The vulnerability curves for the various energy assets and the generalized curve for the energy system are shown in Figure 1.

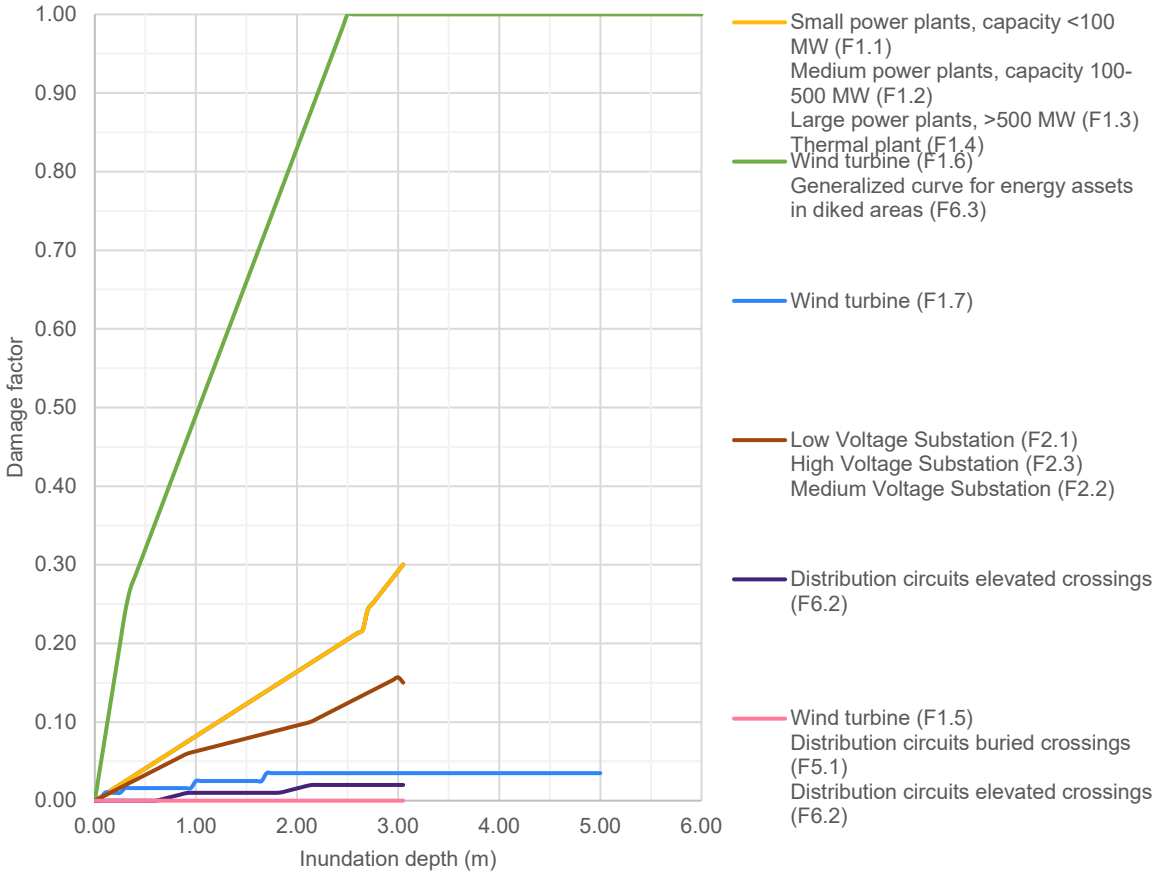

This project has received funding from the European Union's Horizon 2020 research and innovation programme under grant agreement No. 101003598

Figure. 1. *An overview of flood vulnerability curves for energy, both at asset-level and system-level. The ID number (e.g., F1.1) aligns with the numbering of the curves as presented in Nirandjan et al. (2024).*

2.2.2. Transportation

The database consists of 16 vulnerability curves and nine fragility curves for roads, eight vulnerability curves and three fragility curves for railways and three vulnerability curves for airports. For use in raster-based models, Huizinga et al. (2017) provides generalized vulnerability curves for application to the road and railway network in Europe, Asia and at the global scale. The data shows a great variety from which the final curve was constructed; with a max damage value ranging from 0 to 65 €/m^2 that is reached at a water level ranging from 0.5 to 6 m, and a spectrum from smooth incremental curves to curves with one single jump from 0 to 100% of maximum damage. This variety shows that the final smooth exponential curve towards 24 €/m^2 at 6 m water depth hides large variability. An empirical verification by Jongman et al. (2012) confirms this variability, showing that curves well predict damage for one case in Carlisle (United Kingdom), but are very far off for another case in Eilenburg (Germany). We refer to Huizinga et al. (2017) for a complete overview of maximum damages per country.

Van Ginkel et al. (2021) made an object-based translation of these vulnerability data for the European road network, thereby considering specific characteristics for different types of roads (e.g., typical road widths, street lightening). Compared to Huizinga et al. (2017), the first differentiation is that the maximum damage costs are tailored to six different road types in OpenStreetMap (OSM) while correcting for the number of lanes. A second differentiation in the shape of the curve assumes that motorways and trunk roads are located on 1-m high embankments and the other roads on surface level. For motorways and trunks, a third differentiation is made between ‘sophisticated’ vs. ‘simple’ designs, referring to the presence of expensive and vulnerable road accessories such as electronic signalling. A fourth differentiation for all road types is between an upper and lower limit of flow velocities that can reasonably be expected for large-scale river flooding; aiming at use in depth-damage flood models while at the same time acknowledging that flow velocity is at least as important as water depth (Koks et al., 2022; Kreibich et al., 2009). Surprisingly, Van Ginkel et al. (2021) find that an object-translation of the Huizinga et al. (2017) curves result in only slightly lower values, well within the 50% uncertainty interval of the new curves. However, Van Ginkel et al. (2021) also show that with the new curves, much more damage is attributed to motorways and trunks, and much less damage to the other road types. An important limitation of the Van Ginkel et al. (2021) curves is that damage to bridges is completely ignored, whereas empirical research suggests that this can be a major source of damage (Jongman et al., 2012; Koks et al., 2022). The upper- and lower construction costs for motorways, trunk roads, primary roads, secondary roads and other roads in Europe are provided by Van Ginkel et al. (2021). For instance, the construction costs for motorways with 2x2 lanes vary from 3,470 to 34,701 euro/m, depending on the country.

This project has received funding from the European Union’s Horizon 2020 research and innovation programme under grant agreement No. 101003598

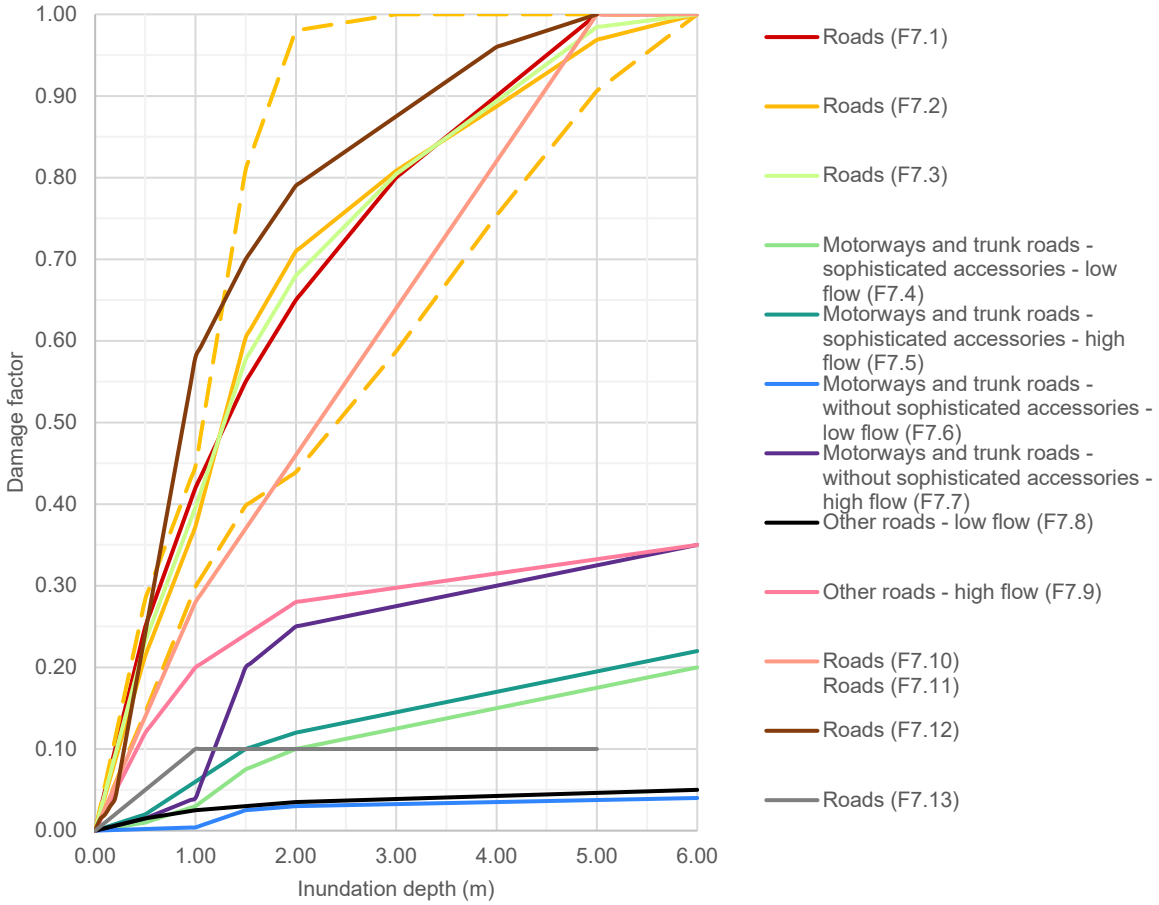

Figure 2. *An overview of flood vulnerability curves for roads. The ID number (e.g., F1.1) aligns with the numbering of the curves as presented in Nirandjan et al. (2024).*

Kok et al. (2005), Vanneuville et al. (2006) and de Bruijn et al (2015) provide a general road, railway and airport curve for application at national scale. Kok et al. (2005) assumes a slowly increasing slope for their curve, reaching a damage of 100% only at an inundation level of 5 m. This function is also used for road and railway risk assessments in Belgium (Vanneuville et al., 2006). The improved version of the aforementioned method is the SSM2015 and contains among others updated damage functions and damage data and are set out in de Bruijn et al. (2015). The updated version of the function assumes a lower vulnerability for water depths under the 25 cm, an increasing vulnerability thereafter due to electric accessories being damaged, followed by a less steeper slope of the curve as additional water is not expected to result in significant additional damage (de Bruijn et al., 2015).

The reconstruction costs for national trunk roads, motorways and other roads in the Netherlands are estimated to be approximately 1,434, 969 and 267 euro/m, respectively. For Belgium, the costs range between the 297 and 7,423 euro/m for roads. The costs for double-tracked railways in the Netherlands is estimated to be 24,883 euro/m, whereas this value is 24,560 euro/m for high-speed railways in Belgium. Also, for Belgium, cost values are based on the number of tracks and whether it is electrified. For single-tracked non-electrified railways, the replacement costs are estimated to be 491 euro/m, whereas it can increase up to 7,368 euro/m for multiple-tracked electrified railways. The construction costs for electrified and non-

This project has received funding from the European Union's Horizon 2020 research and innovation programme under grant agreement No. 101003598

electrified railways in the Netherlands ranges between the 1,335 and 5,344 euro/m. Airports are systems that are composed of multiple elements; the area is covered by (high-value) structural assets such as (un)paved runways, control towers, terminal buildings, aprons, fuel facilities, and maintenance and hanger facilities, but also by low-value elements such as grassland (e.g., in-between runways). For flood risk modelling in Belgium, Vanneuville et al. (2006) distinguishes between an airport area covered by (1) structural elements and (2) without buildings or other significant elements, and provide a maximum damage of 100 euro/m2 and 0 euro/m2 to these categories, respectively. For in the Netherlands, Kok et al. (2005) provide a cost value of 108-129 euro/m2 and de Bruijn et al (2015) a cost value of 114 euro/m2.

Furthermore, the ICPR (2001) propose a generalized road curve for trans-boundary Rhine countries which were constructed using empirical damage data from Germany and expert judgement. The vulnerability curves for roads and airports are presented in Figure 2 and 3, respectively.

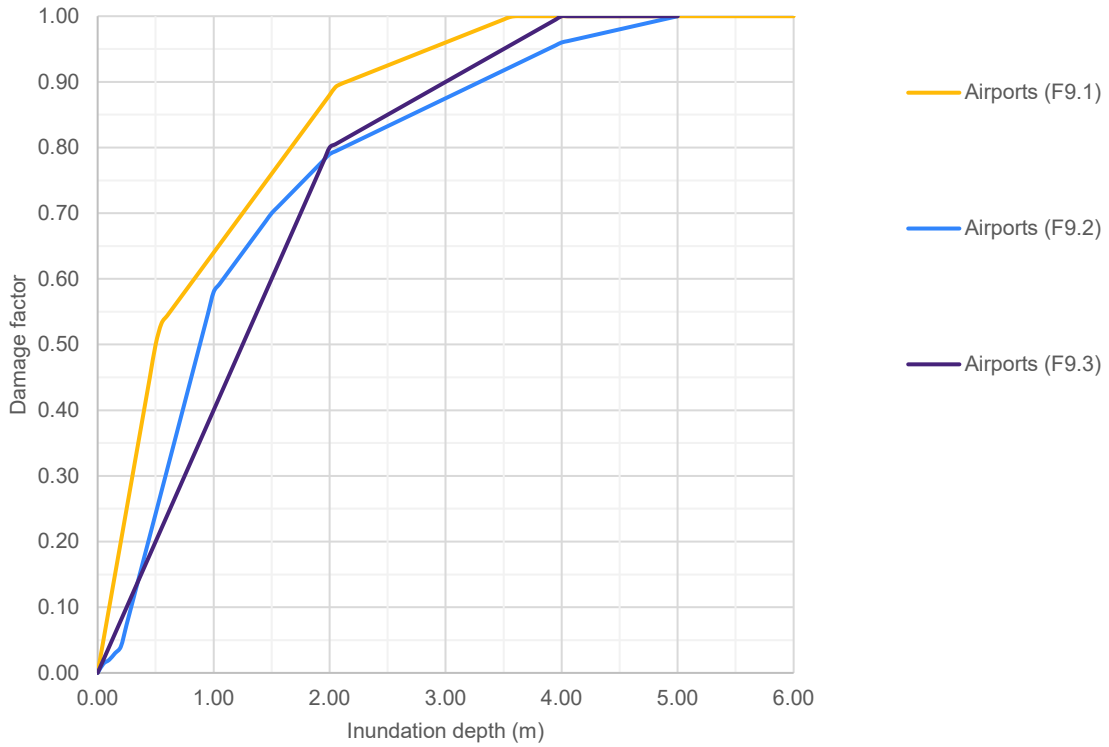

Figure 3. *An overview of flood vulnerability curves for airports. The ID number (e.g., F1.1) aligns with the numbering of the curves as presented in Nirandjan et al. (2024).*

McKenna et al. (2021) developed fragility and vulnerability curves for granular highway embankments through an analytical approach (Figure 4). For their numerical simulations, they expose a highway embankments flood, leading to raised groundwater levels due to moisture ingress, followed by scour hole development at the toe of the embankment slope. The Water Intensity Measure (WIM) is used as an intensity measure to describe the proportion of the embankment height that would be considered saturated if exposed to moisture ingress due to

This project has received funding from the European Union's Horizon 2020 research and innovation programme under grant agreement No. 101003598

flooding. Higher levels of vulnerability and damages are expected with increasing moisture ingress and scour depths.

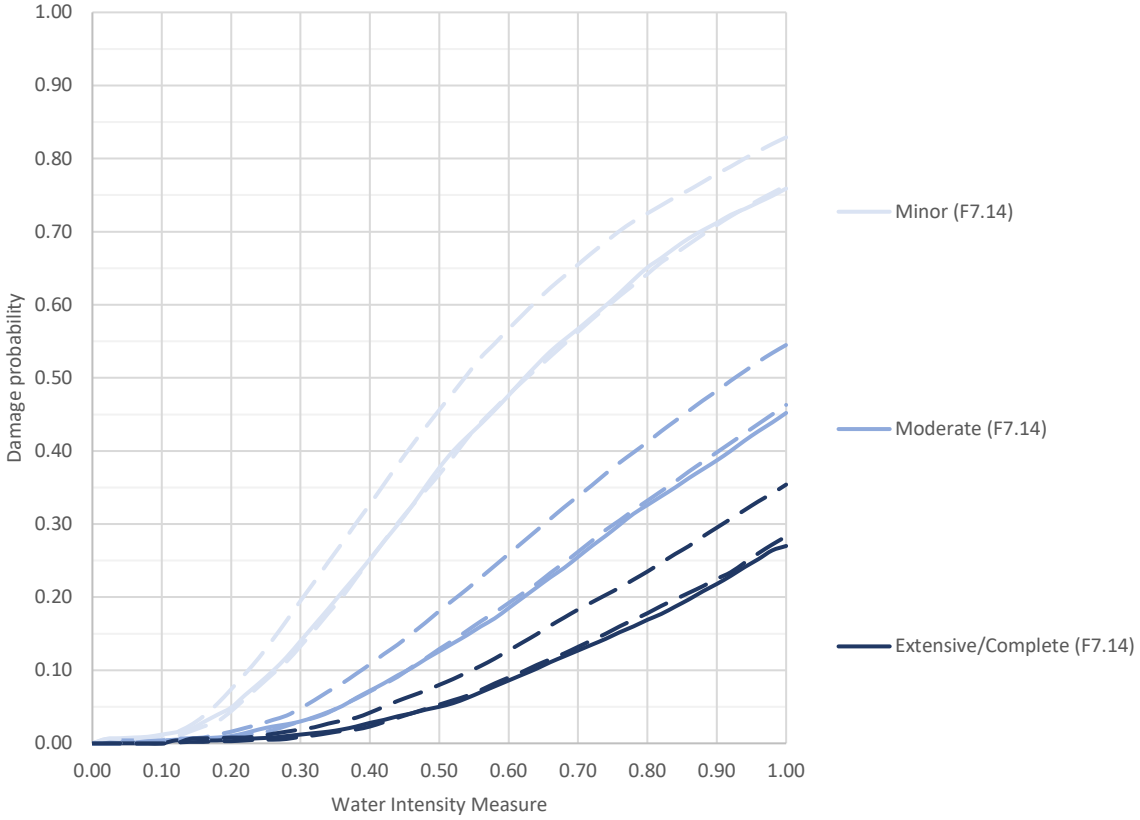

Figure 4. *Fragility curves for granular symmetrical highway embankment with a height of 10 m, a crest width of 10 m, including two traffic lanes of 3.5 m each exposed to moisture ingress (F7.14) and the combined effect of moisture ingress and scour (F7.15) due to flood. The ID number (e.g., F1.1) aligns with the numbering of the curves as presented in Nirandjan et al. (2024).*

This project has received funding from the European Union's Horizon 2020 research and innovation programme under grant agreement No. 101003598

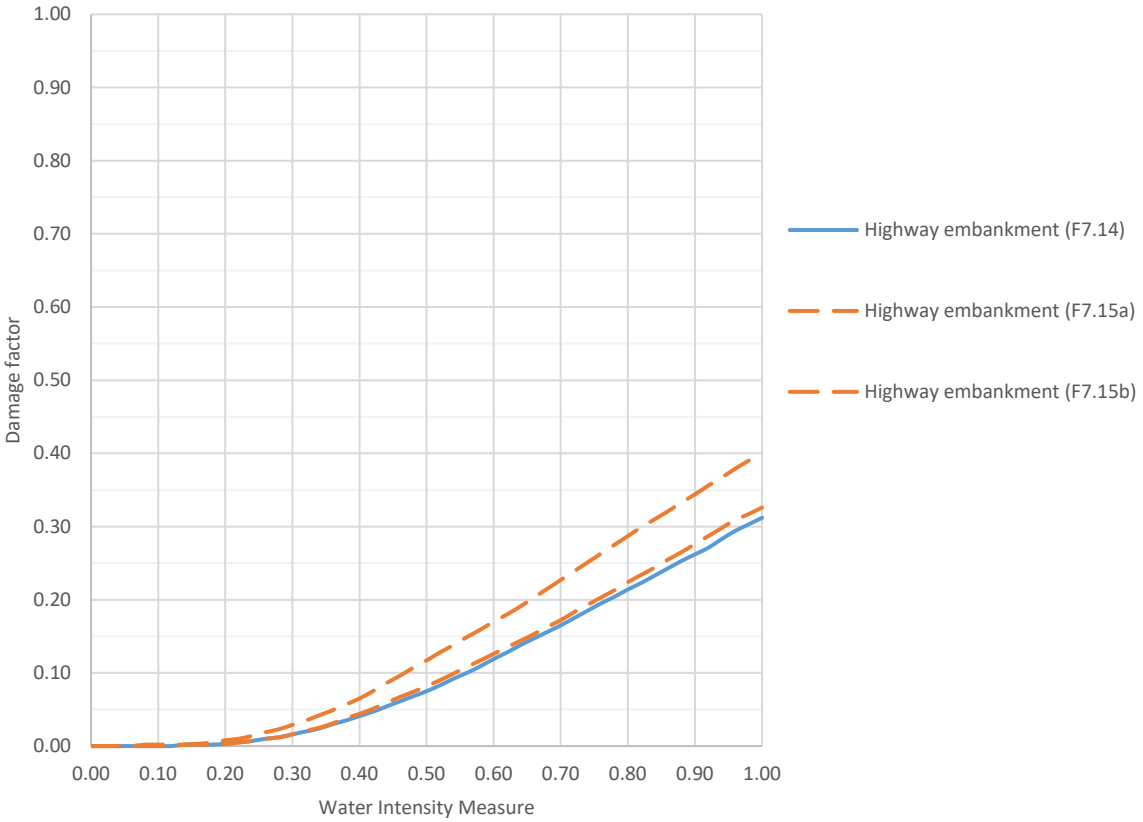

Figure 5. *Vulnerability curves for granular symmetrical highway embankment with a height of 10 m, a crest width of 10 m, including two traffic lanes of 3.5 m each exposed to moisture ingress (F7.14) and the combined effect of moisture ingress and scour (F7.15) due to flood. The ID number (e.g., F1.1) aligns with the numbering of the curves as presented in Nirandjan et al. (2024).*

Kellermann et al. (2015) propose a staircase threshold-wise vulnerability of Austrian railways based on the March River flooding of 2006, whereby photographic documentation of flood damage to a double-tracked Austrian Northern Railway line is used to identify three stages of damage. The railways are assumed to be a standard double-tracked railway cross-section that consists of the following elements: substructure, superstructure, catenary and signals. The first damage class relates to the substructure of the railway that is (partly) impounded by water, but results in only a little damage. The second damage class assumes that the substructure and superstructure of a track segment is completely flooded, which is expected to result in damage to at least the substructure. The final class assumes damage to the superstructure, catenary and/or signals, and that complete restoration is needed for the standard cross-section of the affected track segment. The damage states are linked to damage estimates by correlating hydraulic impacts and damage stages, identifying impact parameters and determining associated thresholds. The derived monetary values for each damage class are used as input for the RAilway Infrastructure Loss (RAIL) model that estimates the direct damages (including repair and cleaning costs) to railway infrastructure due to flooding with low flow velocities (Bubeck et al., 2019; Kellermann et al., 2016, 2015). The maximum damage that can be used

This project has received funding from the European Union's Horizon 2020 research and innovation programme under grant agreement No. 101003598

in combination with this vulnerability curve equals 6,897 euro/m. The vulnerability curves for railways are presented in Figure 6.

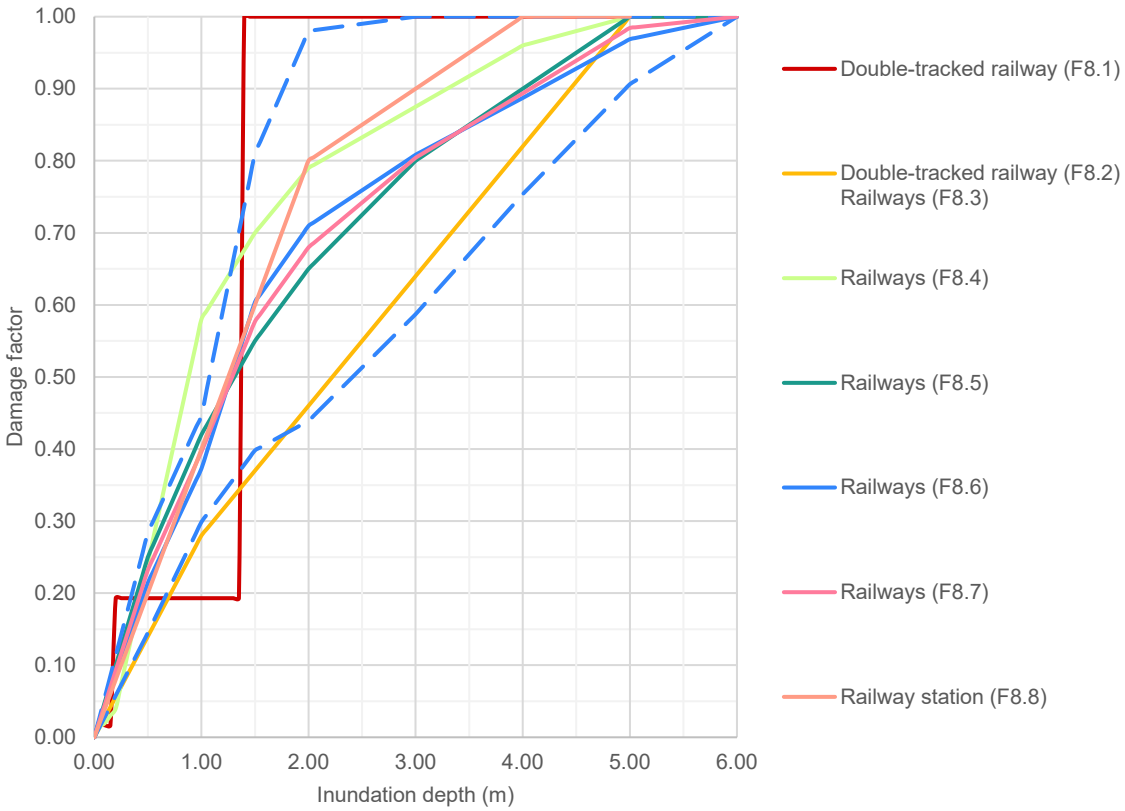

Figure 6. *An overview of flood vulnerability curves for railways. The ID number (e.g., F1.1) aligns with the numbering of the curves as presented in Nirandjan et al. (2024).*

Overtopping due to flooding is a common mechanism that causes damages to railway, which initially starts with scouring of the ballast, which subsequently progresses to scouring of the embankment upon which the rail tracks are built. Using damage records for unelectrified single-track railways of two flood events in Japan, Tsubaki et al. (2016) developed fragility curves for ballast scour damage, embankment fill scour damage and a combination of both damage conditions (Figure 7).

This project has received funding from the European Union's Horizon 2020 research and innovation programme under grant agreement No. 101003598

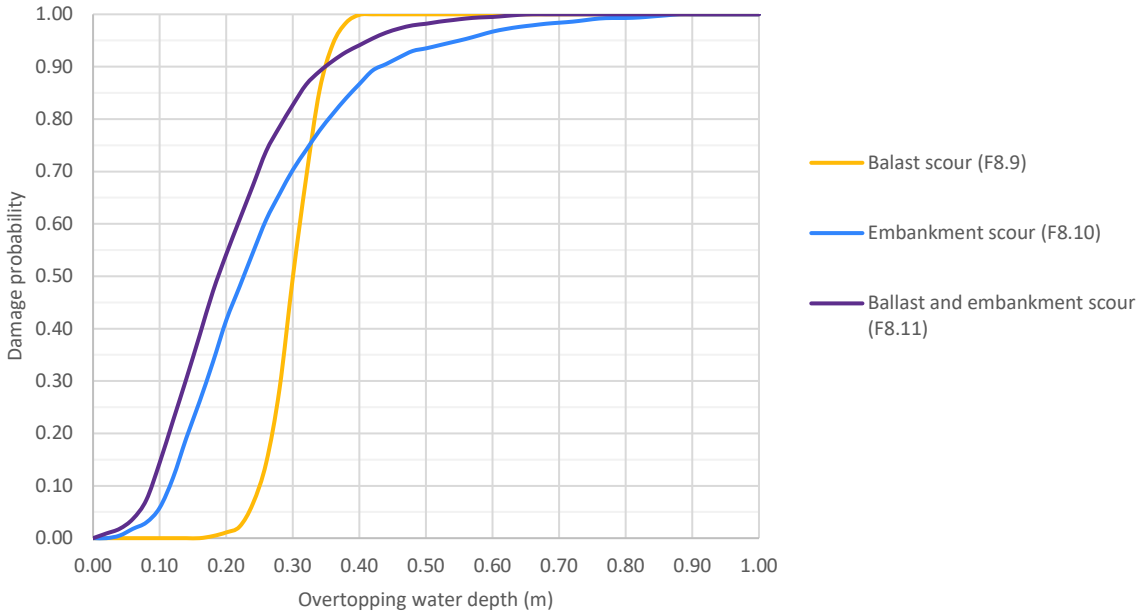

Figure 7. *Fragility curves for single track and non-electrified for three damage conditions. The ID number (e.g., F1.1) aligns with the numbering of the curves as presented in Nirandjan et al. (2024).*

2.2.3. Telecommunication

Only two vulnerability curves for telecommunication assets are found in the current body of literature. Vanneuville et al. (2006) provide a curve for communication towers in Belgium in combination with a cost estimate of 59,202 euro per unit, and Kok et al. (2005) for the overall telecommunication system within dikes areas in the Netherlands. The latter damage function allows for application to high-frequency flooded areas (i.e., return period of higher than 25 years) by adjusting the maximum damage: the maximum damage can be reduced by 25% for risk assessments in these areas as the flood risk is taken account of during the construction phase. The vulnerability curves for telecommunication are presented in Figure 8.

FEMA (2013) formulated a classification for the telecommunication system. This classification includes a range of communication lines and telecom facilities, and determined repair costs for communication lines and replacement costs for the telecom facilities. Fragility curves for these elements, however, will be developed as part of a new technical report on flood risk assessments. Nevertheless, a qualitative measure of the vulnerability of these telecom assets for three measures of flood severity is provided. Switching stations and access vaults are highly vulnerable to inundation, while buried transmission/distribution lines at river crossings are highly vulnerable to scour and erosion processes. A none to medium vulnerability due to debris impact/hydraulic pressure processes is assigned to telecom infrastructure.

This project has received funding from the European Union's Horizon 2020 research and innovation programme under grant agreement No. 101003598

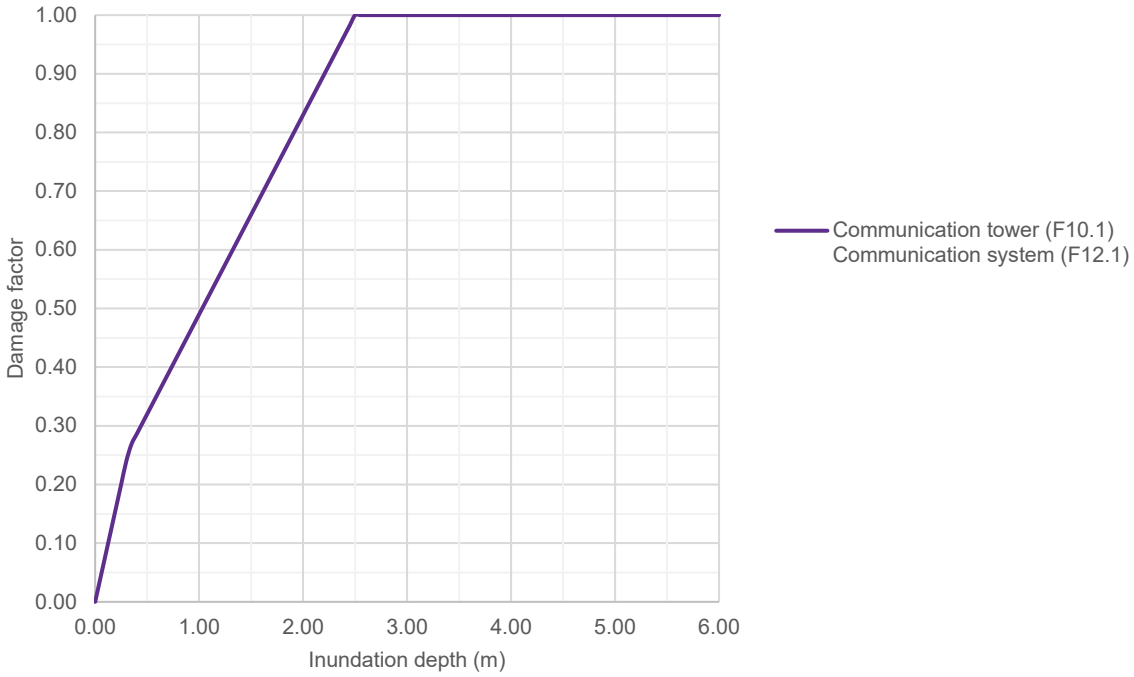

Figure 8. *An overview of flood vulnerability curves for telecommunication, both at asset-level and system-level. The ID number (e.g., F1.1) aligns with the numbering of the curves as presented in Nirandjan et al. (2024).*

2.2.4. Waste

FEMA (2013) provides multiple vulnerability curves for various waste assets. Three damage functions were constructed for three categories of wastewater treatment plant according to capacity: lower than 189 million L/d (i.e., small WWTP), 189-757 million L/d (i.e., medium WWTP), and more than 757 million L/d (i.e., large WWTP). However, the form of the damage function is similar for the three categories of wastewater treatment plants, whereby is assumed that cleanup, repair of small motors, buried conduits and transformers is required from the onset of the flooding. Cleanup and major repair of electrical equipment is required when the flood inundation level exceeds 0.91 m. In addition to these damage functions, damage functions are developed for wastewater treatment plants that have a higher and lower vulnerability. The replacement costs of wastewater treatment plants is estimated to be 124 million euro per unit (FEMA, 2013).

Also, vulnerability curves are provided for sewers and interceptors, control vaults and lift stations. The replacement costs for lift stations are dependent on the capacity of the asset. The replacement costs are 265,818 euro per unit for small pumping plants that have a capacity below 38 million L/day, whereas it is 930,364 euro per unit for medium and large pumping plants that have a capacity between 38-189 L/day and above 189 L/day, respectively. Furthermore, Kok et al. (2005) provides a vulnerability curve for wastewater treatment plants

This project has received funding from the European Union's Horizon 2020 research and innovation programme under grant agreement No. 101003598

within diked areas in the Netherlands. The average cost estimate for wastewater treatment plants is estimated to be 10 million euro per unit, with a wide range starting from 197,874 to 495 million euro per unit. The vulnerability curves for waste assets are presented in Figure 9.

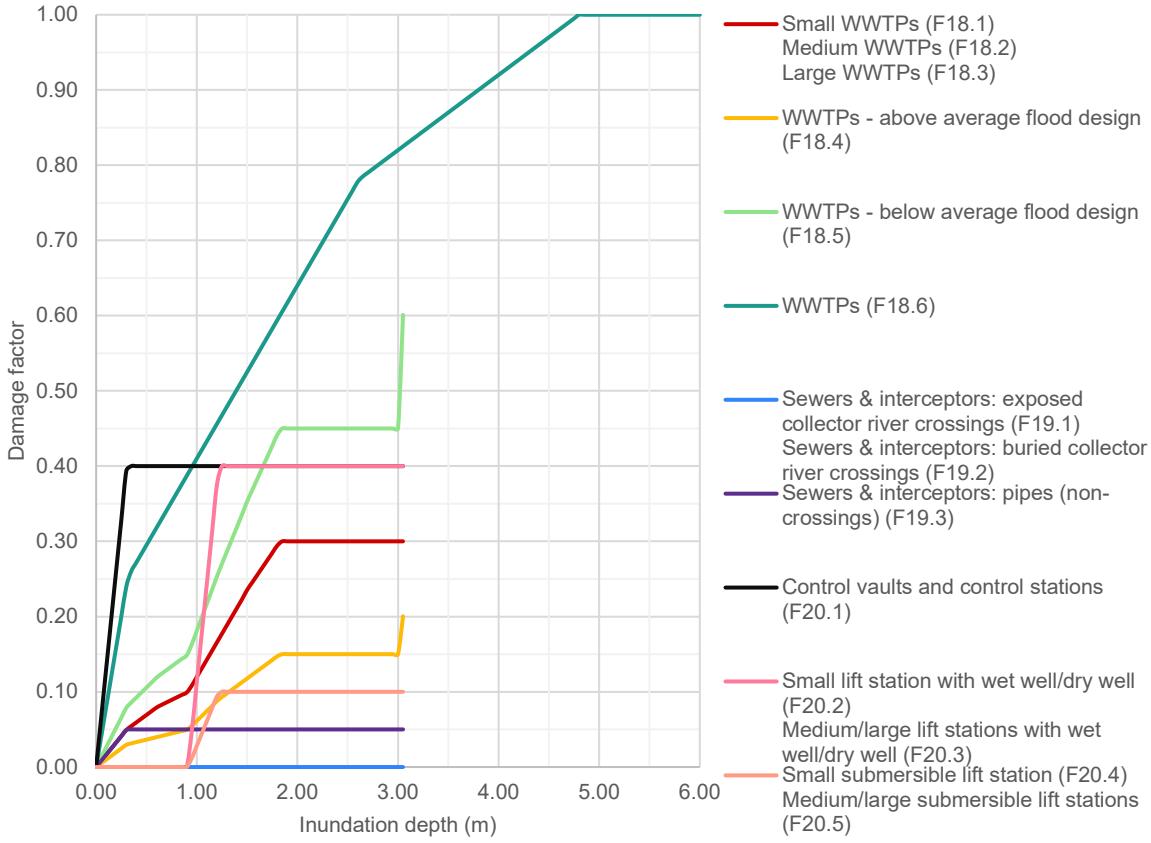

Figure 9. *An overview of flood vulnerability curves for waste assets. The ID number (e.g., F1.1) aligns with the numbering of the curves as presented in Nirandjan et al. (2024).*

2.2.5. Water

FEMA (2013) developed ten vulnerability curves for water treatment plants with various construction designs considering the capacity and whether it is closed or pressurized water treatment plant. Water treatment plants with a capacity of 38-189 million L/day are categorized as small water treatment plants, water treatment plants with a capacity of 189-757 million L/day are categorized as medium water treatment plants, and water treatment plants with a capacity above 757 million L/day are categorized as large water treatment plants (FEMA, 2013). In addition, the building design is taken into account as well, hereby differentiating between designs that are open and closed, and whether they are pressurized. In general, the damage functions for open water treatment plants follow the same curve, and the ones developed for closed and pressurized water treatment plants as well. Here, the damage functions developed for open water treatment plants assume a higher vulnerability compared to the closed and pressurized water treatment plants. Moreover, additional curves are developed for open water treatment plants, and closed and pressurized water treatment plants that represent a less than average damage and a more than average damage. The replacement costs for small, medium

This project has received funding from the European Union's Horizon 2020 research and innovation programme under grant agreement No. 101003598

and large water treatment plants are 26 million, 89 million and 319 million euro per unit, respectively.

FEMA (2013) also presents five vulnerability curves for water storage tanks with varying elevation levels (i.e., at ground level, elevated, or below ground level) and construction materials (i.e., wood, steel, or concrete). The replacement costs vary widely: approximately 1 million euro for concrete water storage tanks at ground level, 709,000 euro for steel water storage tanks at ground level, 27,000 euro for wooden storage tanks at ground level, 709,000 euro for elevated water storage tanks and 1 million euro for water storage tanks below ground level. In addition, vulnerability curves are also developed for pumping plants, control vaults and control stations. For pumping plants, the replacement costs vary depending on the capacity: small pumping plants with a capacity below 38 million L/day have a replacement cost of 132,909 euro per unit, whereas medium and large pumping plants with a capacity above 38 million L/day have a replacement cost of 465,182 euro per unit. The estimated replacement cost for control vaults and control stations equals 44,303 euro. Kok et al. (2005) provides a vulnerability curve for pumping plants with a capacity of 518 L/d in the Netherlands that are in areas with a return period lower than 25 years. For a pumping plant with a capacity of 518 L/day the cost estimate ranges from 49,469 euro per unit to 18 million euro per unit, with an average value of 739,257 euro per unit. Lastly, FEMA (2013) also presents a vulnerability curve for water wells that have a replacement cost of 354,424 euro per unit. The vulnerability curves for water assets are presented in Figure 10 and Figure 11.

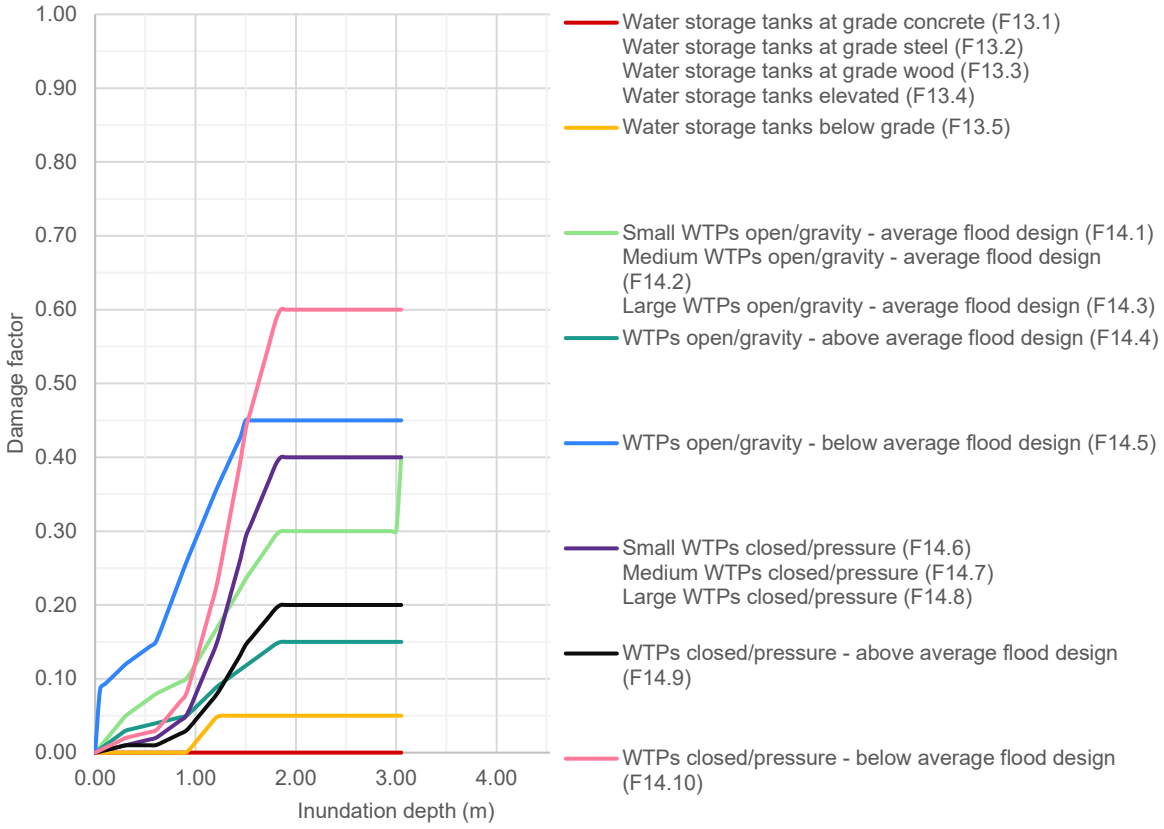

This project has received funding from the European Union's Horizon 2020 research and innovation programme under grant agreement No. 101003598

Figure 10. *An overview of flood vulnerability curves for water storage tanks and water treatment plants (WTPs). The ID number (e.g., F1.1) aligns with the numbering of the curves as presented in Nirandjan et al. (2024).*

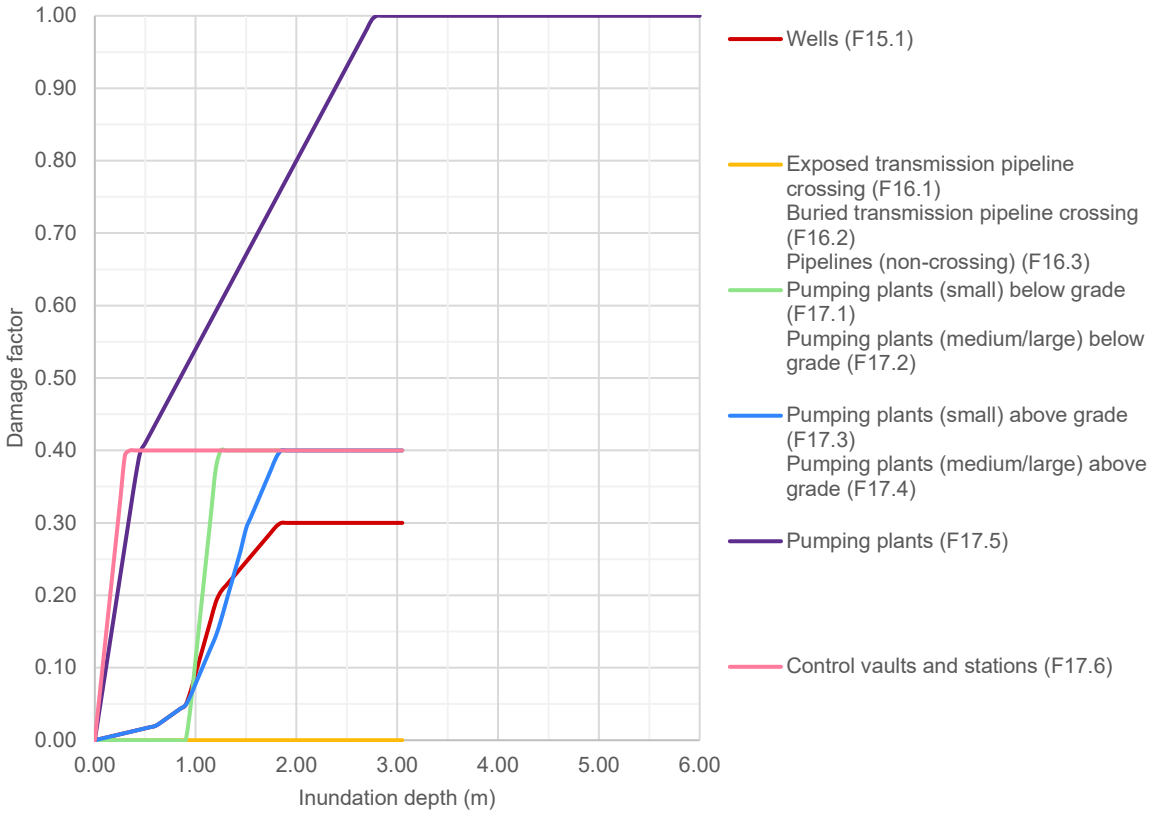

Figure 11. *An overview of flood vulnerability curves for wells, pipelines, pumping plants and control vaults and stations. The ID number (e.g., F1.1) aligns with the numbering of the curves as presented in Nirandjan et al. (2024).*

2.2.6. Education and health

A number of 13 vulnerability curves for education and health facilities are found in the literature. Huizinga et al. (2017) developed continent-specific and global vulnerability data for commercial buildings, which include schools and hospitals as well. In addition, standard deviations are given for the functions that can be applied to Central- and South America, Asia and Oceania, which are useful to set bandwidths for uncertainty analysis. Maximum damages are computed for all countries using regression techniques, and also a world average is presented. In addition to this, maximum damages are provided for building-based risk assessments, land-use based, and object-based, for which we refer to Huizinga et al. (2017).

Kok et al. (2005) presents a generalized vulnerability curve for companies in low-frequency flooded areas and can also be applied to school buildings, whereas de Bruijn et al. (2015) propose one generalized vulnerability curve for educational and health facilities. Vanneuville

This project has received funding from the European Union's Horizon 2020 research and innovation programme under grant agreement No. 101003598

et al. (2006) presents a generalized damage function for buildings that also includes school buildings, and another one for health facilities that are assumed to have a higher vulnerability compared to educational facilities. The maximum damages as presented by de Bruijn et al. (2015) are 983 euro/m^2 for education facilities and 1,953 euro/m^2 for health facilities in the Netherlands. Following Vanneuville et al. (2006), a maximum damage of 1,135 euro/m^2 applies for both hospitals and schools in Belgium. Djordjeviç (2014) developed a damage function for schools in the city of Taipei, Taiwan, using the available literature in combination with field surveys and expert judgement. The maximum damage for school buildings in Taiwan is estimated to be 267 euro/m^2. The same methodology is applied to develop damage functions representing school and health facilities in the municipality of Châtelaillon-Plage located at the Atlantic coast of France (Batica et al., 2018). Here, health facilities are assumed to be more vulnerable to floods compared to education facilities, with the maximum damage of 518 euro/m^2 and 69 euro/m^2, respectively, being reached at a water depth of 3 m. The vulnerability curves for water education and health facilities are presented in Figure 12.

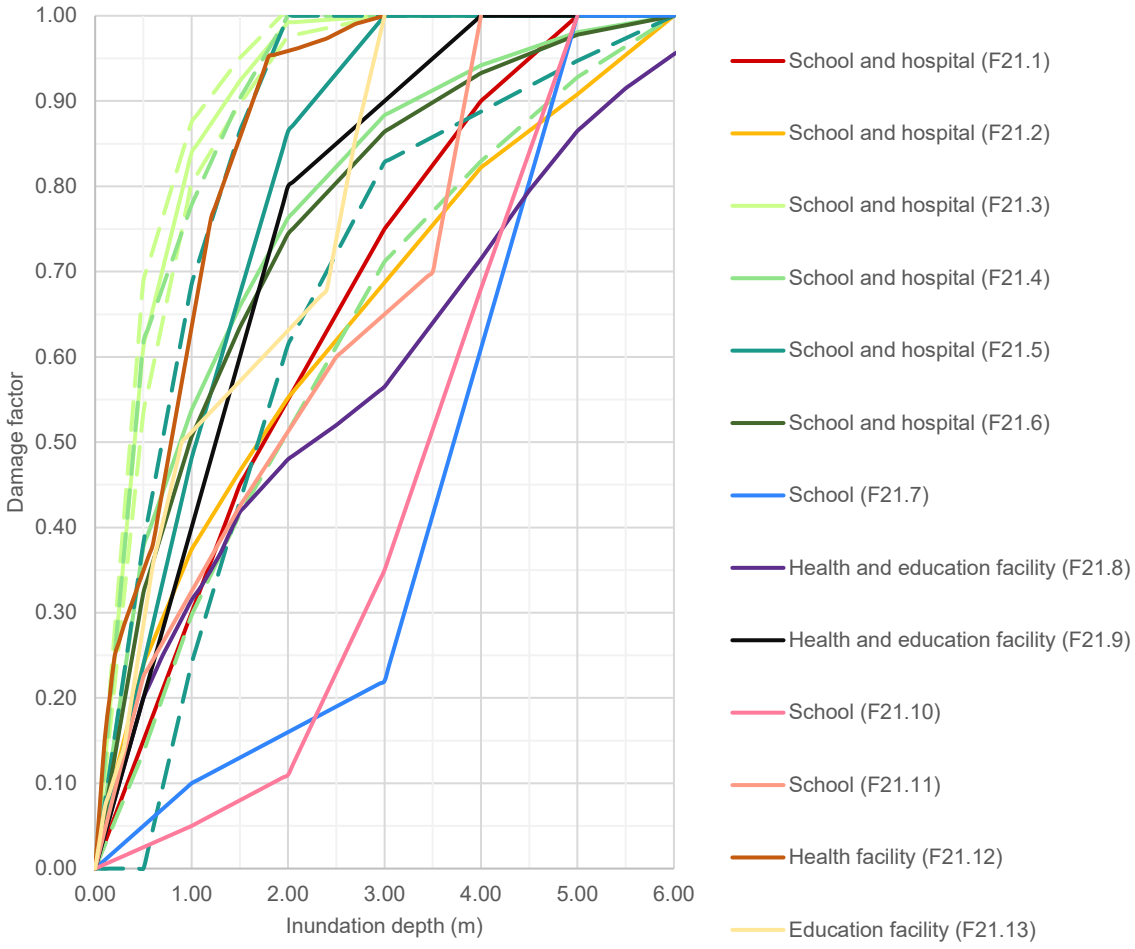

Figure 12. *An overview of flood vulnerability curves for health and education facilities. The ID number (e.g., F1.1) aligns with the numbering of the curves as presented in Nirandjan et al. (2024).*

This project has received funding from the European Union's Horizon 2020 research and innovation programme under grant agreement No. 101003598

2.3. Vulnerability of buildings

Nirandjan et al. (2024) reviewed fragility and vulnerability curves for a specified set of critical infrastructure, including health and educational facilities. Nonetheless, fragility and vulnerability curves are also available for the general building inventory which have been subject of previous research attention, especially within the earthquake domain. There is a limited number of existing open-access databases that focus on structural damages to types of (residential) buildings. For example, the earthquake risk assessment initiatives Global Earthquake Model (GEM) and the Comprehensive Approach to Probabilistic Risk Assessment (CAPRA) platform support an extensive database containing functions for a range of building types (Cardona et al., 2012; Yepes-Estrada et al., 2016).

FEMA (2013) provides damage functions for the general building stock and essential facilities. The general building stock covers five model types which are categorized as wood, steel, concrete, masonry, and mobile homes, which can be further categorized under number of stories and heights. The essential facilities include hospitals (with varying capacities), medical clinics (e.g., clinics, labs, and blood banks), schools (i.e., primary/secondary schools), and colleges/universities (i.e., Community and State colleges, State and Private Universities). Depth-damage functions are provided separately for buildings and contents. The damage to essential facilities can be estimated through default depth-damage functions, which assume a default building type (i.e., brick for schools, concrete for the other facilities), age (i.e., median), and other characteristics (e.g., first floor elevation, building height, and basement). The default depth-damage function can be adjusted to create a specific curve for the building or facility under consideration. These damage functions, however, are only accessible via the HAZUS software, and are thus not included in the database compiled by Nirandjan et al. (2024). For detailed information on this, we refer to the technical flood manual issues by FEMA (2013).

3. Physical & Social vulnerability indicators

3.1. Vulnerability drivers and indicators

Vulnerability indicators are powerful tools to display spatiotemporal variations in vulnerability and to convey this to policy makers or other stakeholders (Abson et al., 2012). Indicators are commonly used in both physical (Papathoma-Köhle, 2016) and social (Fekete, 2019)vulnerability assessments. They require relatively little data compared to alternatives – like vulnerability matrices (e.g., Menoni et al., 2012) or system dynamics models (e.g., Joakim et al., 2016; Zarghami and Dumrak, 2021)

Yet there are also several drawbacks to the use indicators that we need to address. Indicators strongly simplify the complex reality of all that is vulnerability. This is amplified when the indicators are processed into one index, which obscures the underlying vulnerability relationships described by the indicators (Abson et al., 2012; Rufat, 2013; Tapia et al., 2017). Statistical tools like Principal Component Analysis (Abson et al., 2012; Meijer et al., 2023) or fuzzy logic (Araya-Muñoz et al., 2017) can help in this regard by pointing out the most

This project has received funding from the European Union's Horizon 2020 research and innovation programme under grant agreement No. 101003598

influential indicators. Yet, this makes it a data-driven assessment rather than an evidence-based one. In fact, around 85% of vulnerability assessments lack a clear theoretical underpinning (Kuhlicke et al., 2023). Even if there is empirical evidence or a clear theory, one should be aware that empirical evidence of one location is not always transferable to another; the same indicators could have different meanings for different places (Spielman et al., 2020).

Reimann et al. (2024) have tackled some of these issues by creating a gridded global social vulnerability index (GlobE-SoVI), where the importance of each indicator is tested against empirical impact data. Nevertheless, the indicator selection is still largely driven by data availability and provide only a general feel of what makes people vulnerable. For instance, 'education' or 'age' are two indicators that lack details about underlying dynamics that could play a role. Although this works arguable well for a global-level comparison of vulnerability, it lacks the level of detail needed for regional to local scale assessments. We could ask questions like "are all elderly more vulnerable, or only those without social support?", or "What do people with more years of schooling do differently to prepare themselves to a disaster?" A European coastal social vulnerability index for instance would require a collection of local scale data with sufficient empirical evidence to base the indicators on.

We try to tackle this challenge of lacking (empirical) evidence in vulnerability assessments in a two-step process, using (1) evidence-based vulnerability drivers and (2) corresponding vulnerability indicators (Figure 13). We define a vulnerability driver as "a feature that could alter the vulnerability of an urban[1] area to a natural hazard" (Stolte et al., 2024). Note that this is different from a vulnerability indicator, which we view as a measure to operationalize vulnerability (Stolte et al., 2024; Hinkel, 2011). An indicator is thus the operationalization of a driver. For example, whether a business has a coastal flooding disaster plan in place or not partly determines or **drives** its vulnerability to coastal floods. A corresponding **indicator** could be: *the number of businesses within a city which have a coastal flooding disaster plan in place*.

For the drivers, we use VulneraCity (Stolte et al., 2023), the most comprehensive open-source overview of vulnerability drivers in an urban context for six different hazards, among which coastal floods. It contains 360 unique drivers on coastal floods – based on peer-reviewed scientific literature – of which one third is empirically derived. Most of the drivers are about how coastal floods are governed as well as the economic situation in a city. Health and demographic-related drivers appear to be less important for this hazard (Stolte et al., 2024).

We operationalized the coastal flood vulnerability drivers by developing a range of possible vulnerability indicators. To structure this process, we made use of VulneraCity's three-part classification system. Within VulneraCity, Vulnerability dimensions (either physical or social) are the tier with the least amount of detail about the drivers; vulnerability subdimensions provide slightly more detail (11 categories); and vulnerability classes are the tier with the most details (100+ categories). Each dimension contains a set of subdimensions which in turn hold several classes. Each class contains a set of drivers within a similar theme, for instance the class poverty contains drivers on citizen income and affordability of housing, and the class dunes/beaches is on the height of dunes and the presence of beach nourishment among

[1] Although we specifically focus on urban areas here, this definition also applies to rural, peri-urban or any other part of the rural – urban continuum.

This project has received funding from the European Union's Horizon 2020 research and innovation programme under grant agreement No. 101003598

others. We developed a set of indicators per unique combination of hazard, subdimension and class.

The indicators were developed by a group of scholars with demonstrable expertise on vulnerability (De Moel et al., 2015; De Ruiter and Van Loon, 2022; Fekete, 2019; Koks et al., 2023; Reimann et al., 2024; Stolte et al., 2024; Tiggeloven et al., 2020; Ward et al., 2020). Each hazard in VulneraCity was covered by three of the expert vulnerability scholars, again based on their past work (for coastal floods, see for instance Stolte et al., 2024; Koks et al., 2022; Tiggeloven et al., 2020). For each combination of hazard, subdimension and class, a maximum of six indicators per vulnerability expert was allowed, to keep the number of indicators comprehensible: three of them being direct indicators for a driver, and three being proxy indicators. The difference is that direct indicators "are based on data that are directly representative for the vulnerability drivers that are being described" (Stolte et al, in prep.) like in the coastal floods disaster plan example above, whereas proxy indicators "are based on data that are used as a substitute for something that you actually want to measure but for which you don't have direct indicators" (Stolte et al., in prep.) like GDP can be a proxy for adaptive capacity. In total, this practice resulted in a set of 540 unique indicators for coastal flooding.

We further summarized the set of indicators, again for reasons of comprehensibility, by finding common themes between the indicators. This led to a set of 71 aggregate indicators, representing 360 of the 540 unique indicators. We then tried to match these indicators with available supranational-scale urban data (i.e., including data on cities from more than one country). For this, we reviewed over 200 supranational-scale datasets. Datasets were collected by looking through own collections and overviews, next to those of Lindersson et al., (2020), Robin and Acuto (2018) and Ramos and Uitermark (2021). We also performed, snowballing, and focussed internet searches for data that we could not find in the other sources. We tried looking for a systematic approach, but Bahlo and Dahlhaus (2021) show that this is only possible for strongly demarcated research topics and scale. We therefore acknowledge that our review is only semi-systematic, though based on existing overviews of well-known datasets. Data were found for 36 of the 71 aggregate indicators. Additionally, we found eight European (sub)national alternatives for indicators for which we did not find urban-scale data.

In the remaining subsections of this chapter, we will briefly describe some of the most prominent drivers of coastal flood vulnerability (4.2) and subsequently what can be done to operationalize these drivers with the currently available data (4.3).

This project has received funding from the European Union's Horizon 2020 research and innovation programme under grant agreement No. 101003598

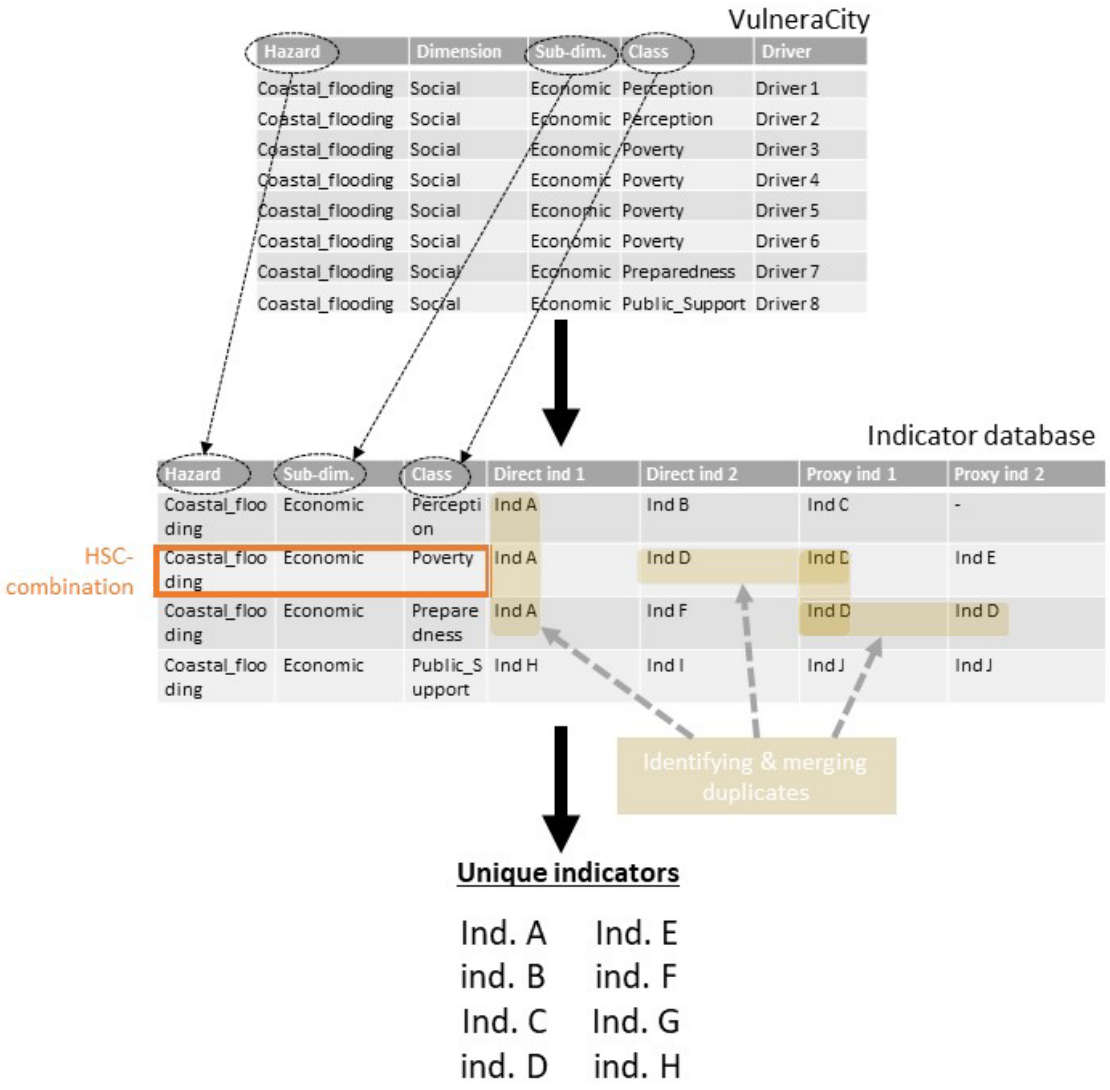

Figure 13. *Flowchart describing the pathway from drivers to indicators. "HSC"-combination stands for a combination of Hazard, Subdimension, and Class. Adopted from: Stolte et al. (in prep.).*

3.2. What drives coastal flood vulnerability?

3.2.1. Physical vulnerability

Analysing the drivers from VulneraCity helps us to understand the mechanics that make people in coastal cities vulnerable to coastal floods. Specifically for critical infrastructure, there are 36 drivers of vulnerability in the database, with two main classes of vulnerability: (1) *Hazard Protection*, which relates among others to hard protection measures like dikes (Lasage et al., 2014; Pinto et al., 2018) or breakwaters (Spiteri and Gauci, 2022), or inland measures like waterproofing utility conduits (Wilson, 2020) or floating pathways (Dal Cin et al., 2021);

This project has received funding from the European Union's Horizon 2020 research and innovation programme under grant agreement No. 101003598

and (2) T*ransport/Traffic*, which deals with the condition of bridges (Qu et al., 2021), ports (Becker et al., 2015), and (evacuation) roads (Fang et al., 2021) for instance. Next to critical infrastructure, there are 74 physical vulnerability drivers for coastal floods, related to general urban assets (mostly associated to drivers about non-critical-infrastructure building use and building material) and the non-human physical environment (e.g., vegetation, beaches and wetlands). We highlight a few examples in the following paragraph.

Alongside major flood protection structures near the coast, flood protection of buildings is a good way to prevent minor floods from entering homes and businesses. Viable options for this are elevating entrances with stepping stones, raising the ground floor of a building, deployable flood protection barriers, or building amphibian/floating buildings (Dal Cin et al., 2021; Frick-Trzebitzky, 2017; Gandini et al., 2020; Lasage et al., 2014; Mycoo, 2014; Spiteri and Gauci, 2022; Wilson, 2020). Flood damage can also be mitigated via architectural choices. Basements or ground floor openings in shops are vulnerable spots in that matter (Gandini et al., 2020). Similarly, intense ground floor usage of buildings can also make them vulnerable to floods; shops and power generators are are less likely to be damaged on the first floor than at the ground floor (Allen et al., 2019). Next to purely anthropogenic measures, flood defences can also come in the form of natural solutions. Vulnerability-lowering options are, among others, salt marshes, barrier islands, dunes, wetland (restoration), and afforestation of foreshores (Gargiulo et al., 2020; Irish et al., 2010; Jonkman et al., 2013; Pinto et al., 2018; van Zelst et al., 2021). This also means that urban development in environmentally-sensitive areas should be contemplated well, as overcrowding such landscapes can lead to lowered protection levels for the city as a whole (Bukvic et al., 2018).

For more information on physical vulnerability drivers of coastal flooding, we refer to our article: Stolte et al., (2024).

3.2.2. Social vulnerability

VulneraCity provides 251 unique indicators on the social vulnerability dimension in an urban context. These are most prominently within the governance, institutional and economic sub-dimensions. Good coastal-flood governance requires close collaboration within the whole coastal region (Chandra and Gaganis, 2016) between governmental institutions, public/private stakeholders, decision makers, engineers and other types of researchers (Spiteri and Gauci, 2022; Allen et al., 2019; Chandra and Gaganis, 2016; Colenbrander and Bavinck, 2017; Jeffers, 2014; Mycoo, 2014). Other important governance drivers are about inclusion of coastal flood risk into urban development planning (Chandra and Gaganis, 2016; de Koning et al., 2019), preferably including future coastal flood or climate change scenarios (Eakin et al., 2021; Jeuken et al., 2015; Wannewitz and Garschagen, 2021).

We found several economic sectors that are either disproportionally impacted by coastal flood or that have disruptive effects on society when hit by a coastal flood event: tourism, coastal restaurants, customer-serving retail, resource extraction industry, fishermen, and farmers (Chandra and Gaganis, 2016; Frick-Trzebitzky, 2017; Meltzer et al., 2021; Mycoo, 2014; Spiteri and Gauci, 2022; Tanir et al., 2021). A city becomes more vulnerable when its economy depends on one or more of these sectors. On the other hand, some sectors actually benefit from coastal flood events, for instance manufacturing and construction firms, which provide materials needed to rebuild any damaged urban assets (Meltzer et al., 2021).

This project has received funding from the European Union's Horizon 2020 research and innovation programme under grant agreement No. 101003598

For more information on social vulnerability drivers of coastal flooding, we refer to our article: Stolte et al., (2024)

3.3. Evidence-based indicators of coastal flood vulnerability

In this section, we will present the evidence-based indicators of coastal flood vulnerability, based on the methods described in Section 4.1. We start off with some summary statistics for all indicators (4.3.1). Next, we describe available and missing data per subdimension from VulneraCity in 4.3.2 (physical vulnerability) and 4.3.3 (social vulnerability). We also use the VulneraCity classes to further describe the data. The classes are denoted in italics and with a Title Case, like *Transport/Traffic*.

3.3.1. Summary statistics

We operationalised our 360 vulnerability drivers from VulneraCity into 540 unique indicators. Note that some drivers share the same indicators, especially in the case of proxy indicators. For each driver, at least one direct or proxy indicator was developed. The 540 indicators were further summarized into 71 aggregate indicators, covering all 11 subdimensions. We then found data from 25 different sources to cover 36 of the 71 aggregated indicators. The 36 covered aggregate indicators trace back to 208 out of the 360 drivers. All the data variables are covering at least some European cities, and 24 of them even have some data for multiple moments in time (temporal dynamics; Figure 14). Altogether this means that we can potentially operationalise 208 drivers of coastal flood vulnerability in a European vulnerability assessment, given the available data.

We should note that the aggregate indicators do not cover all the drivers from VulneraCity. Data may thus exist for the omitted drivers, which is why we only discuss the drivers that are connected to the aggregate indicators in the remainder of this Section. Nevertheless, most vulnerability subdimensions, like General Urban Assets, Health and Environmental, are well covered by both the aggregate indicators and the data (Figure 15). Demographic and Economic stand out for being the least covered subdimensions. For some indicators, we suggest alternative (sub)national data sources if there is no city-level data available.

This project has received funding from the European Union's Horizon 2020 research and innovation programme under grant agreement No. 101003598

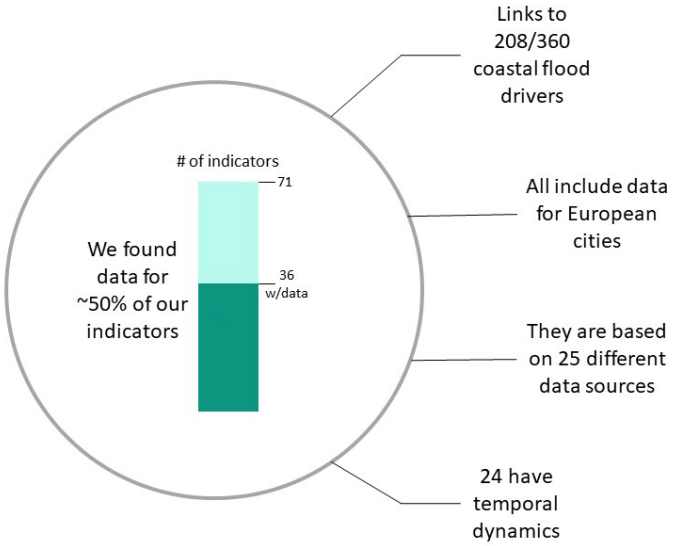

Figure 14. *Summary statistics of our evidence-based indicator collection.*

3.3.2. Physical

We could cover 11 (partially-) physical aggregate vulnerability indicators with the reviewed data. Most of them (6/11) are covered by data from the City Water Optimizer, the City Water Map, OSM or CISI. The remainder of this section goes into more details on what type of data these sources provide. We discuss this per subdimension in decreasing order of their prevalence in VulneraCity.

General Urban Assets

For General Urban Assets, we see good coverage for virtually all classes that are connected to the aggregate indicators (Figure 15). The City Water Optimiser has data on the presence of risk reduction strategies, which indicates that there is some kind of measure implemented to reduce coastal flood risk, but it does not tell us what the exact measure is. Other data variables were a closer fit to the original indicators and drivers, like “Built up surface area” (data variable) is a good fit for “Coverage [area] OR share [percentage] of the built-up area” (original indicator) as a proxy for “Permeable surfaces” (driver). We also found data on *Transport/Traffic* from Eurostat, OSM and the Global Roads Inventory Project. These entail proxy data for the accessibility to main roads (the proxy being “road networks”) and direct indicators for the number of transportation vehicles available. For water source types, we mainly found information on how many households are connected to piped water networks, but we lack information on the alternatives that households use like rain or private wells. We also lack any data for *Building Use*, even though this was a prominent class in VulneraCity (see Section 4.2.1). Data on building conservation status and the attractiveness of protected areas were also absent on the supranational scale.

Table 1. *Indicators and their data sources and related vulnerability classes for the sub-dimension General Urban Assets.*

This project has received funding from the European Union’s Horizon 2020 research and innovation programme under grant agreement No. 101003598

Indicator	Data source (variables)	Related vulnerability classes
Presence [Y/N] OR number of implemented or planned risk reducing measures	City Water Optimizer (Presence of a risk reduction strategy; Presence of implemented land use plans with environmental protection and zoning)	• Detention/Retention • Electricity • Hazard Protection • Other • Transport/Traffic • Urban Development • Building Characteristics
Number of transportation options/vehicles per capita	Eurostat (Number of registered private cars)	• Transport/Traffic
Composition of water sources (per household) by type (e.g., wells, piped, rain)	City Water Optimizer (Percentage of households with access to piped water supply; Percentage of non-residential buildings with access to piped water supply; Share of reclaimed water networks in the city's water system); The City Water Map v2.2 (Type of water sources)	• Water Supply
Share of people that can enter a main road within Xmin (similar to rural accessibility index, RAI) [percentage]	Global Roads Inventory Project (Road network); OSM (Physical objects from OSM)	• Transport/Traffic • Urban Form
Coverage [area] OR share [percentage] of impervious area	The Global Human Settlement Layer (Built up surface area; Long-term built-up land projections)	• Runoff/Infiltration

This project has received funding from the European Union's Horizon 2020 research and innovation programme under grant agreement No. 101003598

Critical Infrastructure

Critical Infrastructure sees a good coverage in *Hazard Protection* from Deliverable 6.1 (the collection of coastal protection standards in Europe) and the City Water Optimiser, but with the same limiting generalisation as mentioned for General Urban Assets. We hardly found any data for *Transport/Traffic* drivers – barring critical infrastructure density from CISI – even though this came forward as one of the most prominent classes of vulnerability drivers to coastal floods in VulneraCity (see Section 4.2.1). There is sufficient data to map critical infrastructure in the flood zone, (if it is combined with flood hazard maps, like from the Coastal Flood Map Catalogue; Dottori et al., 2017, Vousdoukas et al., 2016), but no data to support an analysis of the flood protection level/coverage of critical infrastructure. Similar to General Urban Assets, for which we found no building conservation status information, we did not find data on the status nor the age of roads and bridges. Data on electrical power outages were not found but could potentially be derived from Nighttime Light datasets with some post-processing (Hultquist et al., 2015; Montoya-Rincon et al., 2022). Furthermore, we did not find any information on drainage-(un)clogging practices as well, but we did find direct and proxy indicators for the presence of a centralized waste management system – which could potentially be linked to unclogging activities again.

Table 2. *Indicators and their data sources and related vulnerability classes for the sub-dimension Critical Infrastructure.*

Indicator	**Data source (variables)**	**Related vulnerability classes**
Presence [Y/N] OR number of implemented or planned risk reducing measures	City Water Optimizer (Presence of a risk reduction strategy; Presence of implemented land use plans with environmental protection and zoning)	• Preparedness • Hazard Protection
Share of critical infrastructure in the flood zone [percentage]	CISI (Critical infrastructure's spatial intensity)	• Education • Medical Capacity/Equipment • Transport/Traffic • Waste Disposal
Presence [Y/N] OR coverage [area] of a centralized waste-management/collection system	City Water Optimizer (Percentage of households connected to a sewerage system; Presence of a decentralised water treatment system); The City Water Map	• Drainage • Waste Disposal

This project has received funding from the European Union's Horizon 2020 research and innovation programme under grant agreement No. 101003598

	v2.2 (Level of wastewater treatment)	
Protection level [return periods]	FLOPROS (Flood protection level (coastal and riverine))	• Hazard Protection

Environmental

Environmentally-powered risk-reduction measures can be mapped with the City Water Optimiser. As we saw before, these provide little detail on the exact protective ecosystems in place. Land cover maps like ESA WorldCover, Global Land Cover Share Database, Land Cover CCI could give a bit more detail on the sub-city level on what types of ecosystems, dunes and vegetation are available, but they do not directly link to their protective traits, which is why we did not make this link in our overview. The high-density point clouds from the Subsidence in Coastal Cities dataset do provide sub-city details and can be used to compare subsidence rates within and across cities. Furthermore, CISI and OSM provide proxy indicators for the presence of chemical substances in ports, as they can show the density of chemical businesses there. With this, most of the drivers from Environmental linked to the aggregate indicators are covered by data, even though we did not find data for most of the aggregate indicators. This is possible as many aggregate indicators link back to the same driver(s), but via different indicators as we developed multiple indicators per driver. We only appear to miss data on the "number of buildings OR coverage [area] of development in environmentally sensitive areas", which trace back to the drivers 'Land reclamation' and 'Building in environmentally sensitive or fragile areas'.

Table 3. *Indicators and their data sources and related vulnerability classes for the sub-dimension Environmental.*

Indicator	Data source (variables)	Related vulnerability classes
Presence [Y/N] OR number of implemented or planned risk reducing measures	City Water Optimizer (Presence of a risk reduction strategy; Presence of implemented land use plans with environmental protection and zoning)	• Detention/Retention • Flood Protective Ecosystems • Dunes/Beaches • Hazard Protection • Soil • Vegetation • Water
Presence [Y/N] of subsidence OR average subsidence rate in the city	Subsidence in coastal cities (Land subsidence rate)	• Subsidence/Depressions • Soil • Water

This project has received funding from the European Union's Horizon 2020 research and innovation programme under grant agreement No. 101003598

Number OR share [percentage] of chemical industries/businesses in ports	CISI (Businesses' spatial intensity); OSM (Physical objects from OSM)	• Pollution
Level of topography [score OR index]	USGS (Elevation)	• Subsidence/Depressions • Soil

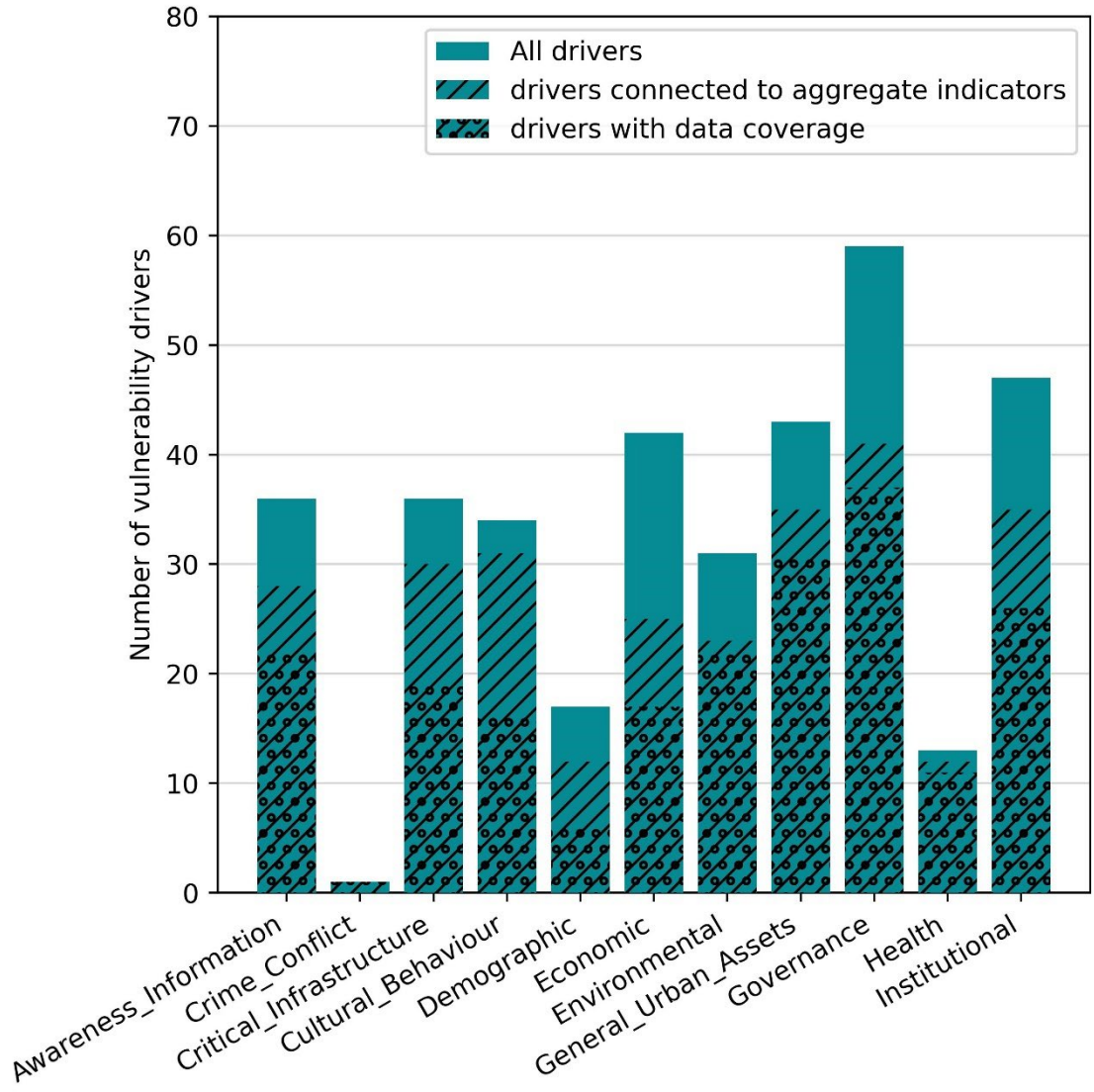

Figure 15. *Bar chart that shows the number of drivers per vulnerability subdimension in VulneraCity, as well as the share of drivers that are connected to the aggregate vulnerability indicators and the ones that we found data for.*

This project has received funding from the European Union's Horizon 2020 research and innovation programme under grant agreement No. 101003598

Social

We could cover 26 unique (partially-)social aggregate vulnerability indicators with the reviewed data. Most of them (18/26) are covered by data from Eurostat, the City Water Optimiser or CDP Cities. The remainder of this section goes into more details on what type of data these sources provide. We discuss this per subdimension in decreasing order of their prevalence in VulneraCity.

Governance

Two important classes in Governance are *Collaboration*, for which there are hardly data available, and *Planning* for which there are relatively much data. Interestingly, we did not find data for the Institutional *Planning* drivers. Governance *Planning* data come from the City Water Optimiser, ESA WorldCover and Land Cover CCI. The latter two provide proxies of the change in wetlands coverage via temporally dynamic land cover maps. The different maps from the ESA WorldCover are derived from different sources though and one should be careful when comparing them. As discussed for the physical subdimensions, the City Water Optimizer does not provide any details on the type of flood protection measures, which is unfortunate for the physical subdimensions, but which provides just the right amount of information for Governance. For collaboration, the CDP Cities database provides descriptions of citizen/stakeholder engagement in coastal flood risk adaptation projects. Note that this does not necessarily provide us with the complete picture of stakeholder engagement in a city, as potentially not all the coastal flood risk adaptation projects of a city are in the database. Furthermore, we found perceptions of corruption in public administration coming from questionnaires conducted by Eurostat. We did not find data for the type of government in a city, which is a proxy for many governance drivers, like disaster justice, the ability to attract external financial aid, political stability, and clientelism. We also could not find any information on the returns of multi-purpose investments nor about the presence of official post-disaster guidance.

Table 4. *Indicators and their data sources and related vulnerability classes for the sub-dimension Governance.*

Indicator	**Data source (variables)**	**Related vulnerability classes**
Level of corruption [score OR index]	Eurostat (Level of corruption in public administration)	• Legal Procedures • Politics • Willingness To Take Action
Presence [Y/N] OR number of implemented or planned risk reducing measures	City Water Optimizer (Presence of a risk reduction strategy; Presence of implemented land use plans with	• Other Policies • Planning • Politics • Resource Allocation • Risk Management • Urban Development • Willingness To Take Action

This project has received funding from the European Union's Horizon 2020 research and innovation programme under grant agreement No. 101003598

	environmental protection and zoning)	
Presence [Y/N] OR number of policies or planning documents to reduce coastal flood risk	City Water Optimizer (Presence of climate change-induced water risks in adaptation planning documents; Presence of a risk reduction strategy; Presence of a risk map for the hazards threatening the city; Presence of water-risks related early warning system(s); Presence of implemented land use plans with environmental protection and zoning; Presence of policies on the protection of critical aquatic habitats & ecosystems)	• Other • Other Policies • Planning • Public Support • Risk Management • Urban Development
Number OR share [percentage] of stakeholders involved in coastal flooding management projects	CDP Cities database (Number and type of stakeholders engaged in adaptation)	• Collaboration • Empowerment
Presence of citizen involvement in coastal flooding management [Y/N]	CDP Cities database (Number and type of stakeholders engaged in adaptation)	• Collaboration • Empowerment • Incentives • Perception
Coverage [area] of wetlands that are converted to built-up area or vice versa	ESA WorldCover (Land cover); Land Cover CCI (Land cover)	• Planning • Urban Development

This project has received funding from the European Union's Horizon 2020 research and innovation programme under grant agreement No. 101003598

Institutional

There is some overlap between Governance and Institutional indicators, since they are closely linked concepts. Most overlapping indicators are covered by data, barring "type of government" (which was also not covered for Governance). Most of the data for this subdimension links back to Institutional *Preparedness. T*he CDP Cities database provides numbers on the public spending on coastal flood protection measures. Combined with a city's GDP, we can estimate how much of their budget they spend on hazard protection. Note that this does not necessarily provide us with the complete picture of stakeholder engagement in a city, as potentially not all the coastal flood risk adaptation projects of a city are in the database. Most other finance-related indicators are lacking data though. We did not find any information on taxes in cities, so we could not compare the level of wealth vs the height of taxes. One could resort to the national-scale GDP-to-tax ratio from Eurostat as an alternative though. Furthermore, there was no data on external (financial) support to cities nor was there anything on the height of environmental-law violation fines. Lastly for Institutional, we miss data on how many coastal flood related personnel is available in resilience building institutes.

Table 5. *Indicators and their data sources and related vulnerability classes for the sub-dimension Institutional. Greyed-out rows indicate that there are non-urban scale data available for an indicator.*

Indicator	**Data source (variables)**	**Related vulnerability classes**
Presence [Y/N] OR number of implemented or planned risk reducing measures	City Water Optimizer (Presence of a risk reduction strategy; Presence of implemented land use plans with environmental protection and zoning)	• Gathering/Conveying Information • Ignorance • Incentives • Perception • Preparedness • Role Clarity • Urban Development
Level of corruption [score OR index]	Eurostat (Level of corruption in public administration)	• Hazard Protection • Incentives • Perception • Resource Allocation • Role Clarity • Trust
Presence [Y/N] OR number of policies or planning documents to reduce coastal flood risk	City Water Optimizer (Presence of climate change-induced water risks in adaptation	• Education • Gathering/Conveying Information • Incentives • Institutional Capabilities • Insurance/Security

This project has received funding from the European Union's Horizon 2020 research and innovation programme under grant agreement No. 101003598

	planning documents; Presence of a risk reduction strategy; Presence of a risk map for the hazards threatening the city; Presence of water-risks related early warning system(s); Presence of implemented land use plans with environmental protection and zoning; Presence of policies on the protection of critical aquatic habitats & ecosystems)	• Preparedness • Public Support
Public spending on coastal flooding management [percentage of city's GDP]	CDP Cities database (Costs of adaptation projects); Global Metro Monitor (GDP in PPP; GDP per capita); Metropolis (GDP per capita)	• Knowledge/Expertise • Other • Preparedness • Risk Management • Willingness To Take Action
Level of wealth [score OR index] vs taxes [monetary amount]	Eurostat (There are data on a national-scale level on the tax-to-GDP ratio)	• Poverty • Public Support

Economic

Although there are many different sources with economic data (Global Metro Monitor, Gridded global datasets for Gross Domestic Product and Human Development Index, OECD stats / City Statistics, and Eurostat), they link mostly back to drivers on *Occupation* and *Economic Profiles* of cities. We also found GDP data and data on past spendings on coastal flood adaptation, which serve as proxies for *Resource Allocation* (both), *Investments/Savings* (past spendings), and *Business Characteristics* (GDP) to name a few classes. There are data on both the composition of the population and the GDP produced per economic sector. This is not made spatially explicit on the sub-city scale, so we cannot say how much of the city's

This project has received funding from the European Union's Horizon 2020 research and innovation programme under grant agreement No. 101003598

economy is located in the flood zone. However, one could take land cover (e.g., from Corine) and a flood map (e.g., the Coastal Flood Map Catalogue; Dottori et al., 2017; Vousdoukas et al., 2016) to estimate the share of industry in the flood zone. A lack of housing prices data makes that we cannot compare prices in and outside the flood zone. It would also be good to have data on how many people are insured against coastal floods, to indicate how well the recovery process in the post-disaster phase would be. Lastly, the dependency of the city on external resources is again difficult to monitor (as with Governance and Institutional) as we do not have data on the city (or its citizens') remittances.

Table 6. *Indicators and their data sources and related vulnerability classes for the sub-dimension Economic.*

Indicator	**Data source (variables)**	**Related vulnerability classes**
Composition of population by economic sector	Eurostat (Distribution of the population per economic sector)	• Economic Profile • Occupation
City's GDP [timeseries]	Global Metro Monitor (Employment change); Gridded global datasets for Gross Domestic Product and Human Development Index (GDP PPP); OECD stats / City Statistics (GDP per capita)	• Business Characteristics • Occupation • Poverty • Resource Allocation
Past spendings on coastal flooding adaptation [monetary amount per year]	CDP Cities database (Costs of adaptation projects)	• Investments/Savings • Perception • Preparedness • Resource Allocation
Composition of the city's income by economic sector	Eurostat (Gross value added at basic prices per economic sector)	• Economic Profile • External Support • Occupation

This project has received funding from the European Union's Horizon 2020 research and innovation programme under grant agreement No. 101003598

Awareness & Information

This subdimension has data for six out of nine aggregate indicators. Coastal flood frequency is well covered with four different data sources. Many other indicators are covered by the City Water Optimiser again, with several variables on collaboration between water-related stakeholders. The public perception survey from Eurostat provides information on the level of trust in the government. For Governance and Institutional, the level of corruption was also based on this survey, but for corruption one could argue that there are other metrics to measure it more directly, whereas the level of trust in the government is actually directly measured by this type of survey. This is a good example where the same type of data is more applicable to one vulnerability indicator or subdimension than another. We lack information on how many people have access to centralized knowledge databases on coastal flood risk and how many people receive risk information in the first place, but technically each citizen of European cities should have access to the Copernicus Emergency Management information in case of a disaster. Furthermore, there was no data on social polarization, which can be used to indicate the level of trust that people put in risk information distributed via official channels.

Table 7. *Indicators and their data sources and related vulnerability classes for the sub-dimension Awareness & Information. Greyed-out rows indicate that there are non-urban scale data available for an indicator.*

Indicator	**Data source (variables)**	**Related vulnerability classes**
Frequency of coastal flooding [number of occurrences over the past X years]	Global Active Archive of Large Flood Events (Frequency of flooding); The Global Flood Database (Frequency of flooding); The Global Flood Monitor (Frequency of flooding); EM-DAT (Frequency of flooding)	• Experience • Perception • Awareness • Gathering/Conveying Information
Presence [Y/N] OR reach [number of people that receive early warnings/forecasts] of a flood	City Water Optimizer (Presence of water-risks related early warning system(s))	• Experience • Gathering/Conveying Information • Monitoring • Preparedness

This project has received funding from the European Union's Horizon 2020 research and innovation programme under grant agreement No. 101003598

forecast/Early Warning System		
Level of trust in the government [score OR index]	Eurostat (Level of trust in public administration)	• Other • Trust
Presence [Y/N] OR number of implemented or planned risk reducing measures	City Water Optimizer (Presence of a risk reduction strategy; Presence of implemented land use plans with environmental protection and zoning)	• Planning • Experience • Gathering/Conveying Information
Level of institutional or stakeholder engagement [score OR index]	City Water Optimizer (Collaboration & co-ordination; Level of collaboration between water-related agencies; Level of collaboration between upstream and downstream stakeholders; Presence of collaboration between sectors on water use and reuse)	• Collaboration • Gathering/Conveying Information
Presence [Y/N] OR reach [number of people that receive the information] of risk communication	Copernicus Emergency Management Service (EU citizens can find detailed geospatial information on this platform, so theoretically, this should be the same for all cities).	N/A

This project has received funding from the European Union's Horizon 2020 research and innovation programme under grant agreement No. 101003598

Cultural & Behaviour

This subdimension lacks data for about half of the drivers that are connected to the aggregate indicators, even though we found data for most of the aggregate indicators. The indicators for which we have no data contain many individual drivers, especially for the aggregate indicators "Number OR share [percentage] of people with access to (un)official social support" and "Type of society [e.g., individualism vs collectivism; cultural mode; religious mode]". There is national-scale data on social contacts from Eurostat though. Furthermore, Eurostat's public perception survey could provide some insights in these type of indicators with data on people's perception on the helpfulness of public administration services. As with the physical vulnerability subdimensions, the presence of implemented/planned risk reducing measures are only telling part of the story, as there is no information on specific risk reducing behaviour, like preparing emergency supplies or digging floodwater diversion channels. We did find some information on physical objects that tell us something about people's behaviour though. OSM provides location of cultural heritage sites and, when combined with permanent water body data, can also tell us something about how many citizens live close to water. Lastly for this subdimension, the GINI index gives an estimation on the composition of wealth by households.

Table 8. *Indicators and their data sources and related vulnerability classes for the sub-dimension Cultural & Behaviour. Greyed-out rows indicate that there are non-urban scale data available for an indicator.*

Indicator	**Data source (variables)**	**Related vulnerability classes**
Presence [Y/N] OR number of implemented or planned risk reducing measures	City Water Optimizer (Presence of a risk reduction strategy; Presence of implemented land use plans with environmental protection and zoning)	• Adaptive Behavior • Drainage • Hazard Protection • Mobility • Other • Preparedness • Incentives • Perception
Number OR share [percentage] of people living close to water (specifically the sea and attachted waterbodies)	Global 3-second Water Body Map (Permanent water bodies; Seasonal water bodies); OSM (Physical objects from OSM); Water Bodies Collection 300m, v. 1 (Permanent water bodies; Seasonal	• Health Affecting Behaviour

This project has received funding from the European Union's Horizon 2020 research and innovation programme under grant agreement No. 101003598

	water bodies); Global Surface Water (Permanent water bodies; Seasonal water bodies)	
Number OR coverage [area] of cultural heritage buildings or sites	OSM (Physical objects from OSM)	• Hazard Protection • Religion
Composition of wealth by households	City Prosperity Index (Gini Coefficient)	• Drainage • Poverty
Presence [Y/N] OR number of social contacts within the city	Eurostat (There is national-level data on the share of persons having contacts with family (relatives) or friends by sex, age, educational attainment and frequency)	• Adaptive Behavior • Connections • Public Support • Social Support

Demographic

This is one of the smaller subdimensions for coastal flood and it also has a low data coverage. Yet, we covered all indicators but two with data. The lack of data on (ethnic) minorities is the main reason for the relatively low coverage. This links back to drivers as “Linguistic barrier”, “Minority groups”, and “Race”, relating to the second-class status that most minorities experience. Eurostat has some national-scale data on the composition of the population by country of birth though, but we should beware that the situation in a specific city could be very different from the country’s average. Eurostat also provides some city-level data covering for the composition of the population by educational direction, tenants VS homeowners, share of citizens with access to quality housing, and the level of corruption. Furthermore, CISI and OSM could be used to find out the density of grocery stores which is important to indicate the availability of food stores in the neighbourhood.

Table 9. *Indicators and their data sources and related vulnerability classes for the sub-dimension Demographic. Greyed-out rows indicate that there are non-urban scale data available for an indicator.*

This project has received funding from the European Union’s Horizon 2020 research and innovation programme under grant agreement No. 101003598

Indicator	Data source (variables)	Related vulnerability classes
Composition of population by educational direction (e.g., theoretical, practical, with or without graduate degree)	Eurostat (Education distribution (over the working age population)	• Education
Number of tenants vs homeowners [ratio]	Eurostat (Number of households owning their dwelling; Number of households in social housing; Number of households in private rented housing)	• Homeowners/Tennants
Number OR density of grocery stores	CISI (Buildings' spatial intensity; Businesses' spatial intensity); OSM (Physical objects from OSM)	• Food
Number OR share [percentage] of the population with access to quality housing	Eurostat (Number of dwellings without basic amenities)	• Poverty
Level of corruption [score OR index]	Eurostat (Level of corruption in public administration)	• Public Support
Number OR share [percentage] of (ethnic) minorities	Eurostat (there is national-scale data on the share of the population by country of birth)	• Minorities/Outsiders • Others

This project has received funding from the European Union's Horizon 2020 research and innovation programme under grant agreement No. 101003598

Health

Almost all Health-related drivers are covered by the data, even though we only have data for four out of eight aggregate indicators. Many drivers overlap with the different indicators. For instance the driver “compromised health” can be measured with the indicators “Composition of population by age”, “Level of healthcare [score OR index]”, and “Share of the population with access to healthcare [percentage]”. Nevertheless, we lack specific information on how many people have access to medication/healthcare, how many are chronically ill, and how affordable healthcare is, although this information is available on a (sub)national scale. The indicators for which we do have data are on a more generalised level: level of healthcare, composition of the population by age (indicating how many physically-vulnerable people there are), and number or share of chemical industries in the flood zone (indicating how much dangerous chemicals there are in danger of flowing into residential areas during a flood).

Table 10. *Indicators and their data sources and related vulnerability classes for the sub-dimension Health. Greyed-out rows indicate that there are non-urban scale data available for an indicator.*

Indicator	**Data source (variables)**	**Related vulnerability classes**
Number of households x days for which there is no clean water	City Water Optimizer (Level of water service continuity)	• Sanitation • Water Supply • Water Treatment
Level of healthcare [score OR index]	Eurostat (Self-perceived healthcare quality)	• Compromised Health • Health Affecting Behaviour • Medical Capacity/Equipment • Other • Sanitation
Composition of population by age	Eurostat (Distribution of the population in age groups)	• Compromised Health
Number OR share [percentage] of chemical industries/businesses in the flood zone	CISI (Businesses' spatial intensity)	• Contamination
Number OR share [percentage] of chronically-ill,	Eurostat (there are subnational-scale data on the	• Compromised Health • Other

This project has received funding from the European Union’s Horizon 2020 research and innovation programme under grant agreement No. 101003598

disabled, or immobile citizens	prevalence of disability among inhabitants)	
Presence of [Y/N] OR number OR share [percentage] of people with access to medication	Eurostat (there are national-scale data on self-reported unmet needs for medical examination with the main reason declared. One possible reason is 'too expensive')	• Medical Capacity/Equipment

Crime & Conflict

This is the smallest subdimension with only one driver attached to it: Law enforcement. This one is covered to some extent by the presence of implemented or risk reducing measures. It is a proxy for law enforcement, as it is likely that the authorities want to enforce measures when they are implemented on a large scale to ensure that their investments are not lost. Some more concrete, yet national-scale, data on law enforcement is also available via Eurostat.

Table 11. *Indicators and their data sources and related vulnerability classes for the sub-dimension Crime & Conflict. Greyed-out rows indicate that there are non-urban scale data available for an indicator.*

Indicator	**Data source (variables)**	**Related vulnerability classes**
Presence [Y/N] OR number of implemented or planned risk reducing measures	City Water Optimizer (Presence of a risk reduction strategy; Presence of implemented land use plans with environmental protection and zoning)	• Regulation

This project has received funding from the European Union's Horizon 2020 research and innovation programme under grant agreement No. 101003598

Presence of law enforcement [Y/N]	Eurostat (There is national-scale data on the number of persons brought before criminal courts by legal status of the court process	• Regulation
Number OR share [percentage] of citizen arrests	Eurostat (There is national-scale data on the number of suspects and offenders)	• Regulation

3.4. From indicators to index: common methods

Collecting evidence-based indicators is only one piece of the vulnerability puzzle. Before deriving an index from them, several choices need to be made regarding further indicator selection (i.e., relevance for the target audience and testing for multicollinearity), standardisation and weighting of indicators, and type of index among others. The most common methods to derive an index are deductive, inductive, vulnerability profiling, and hierarchical vulnerability assessments, each of which we will briefly discuss here.

The inductive approach starts by collecting all possibly relevant vulnerability indicators (usually at least twenty indicators; for instance based on our overview), after which they use statistical analysis, mostly done by Principal Component Analysis (PCA), to determine which indicators are uncorrelated and explain most of the variance in the data (Tate, 2012; Yoon, 2012) These are then all combined into a single index or number. The deductive approach, on the other hand, uses a relatively small (~10) set of indicators that are pre-selected based on literature and expert judgement, instead of statistical analysis like in the inductive approach (Tate, 2012; Yoon, 2012). Vulnerability profiling starts similar to the inductive approach, with statistically reducing a large set of indicators. It then requires a classification of several vulnerability (sub)dimensions (like Stolte et al. (2024) did in VulneraCity) for which one dominant indicator is selected per class. The relative vulnerability of each class is assessed by analysing their spatial patterns (Rufat, 2013). Lastly, hierarchical models are like deductive approaches in that they require a preselection of indicators, but also like vulnerability profiling in that they distribute them into subgroups of vulnerability (Savelberg et al., in review). Each method has benefits and drawbacks. For instance, the inductive approach is useful for data rich regions for which there is not much known about the context of the area or if the area is large (continental scale), because it is mainly data driven. When more context is available, the inductive approach may become less useful and the deductive or hierarchical models become interesting options, as there may be sufficient context to inform which indicators to use. Vulnerability profiling becomes useful when the end user wants to have information on relative vulnerability per class and less in what the overall vulnerability of a place is (which is arguably also impossible to derive as we discussed in Section 4.1). We should note that the choice of

This project has received funding from the European Union's Horizon 2020 research and innovation programme under grant agreement No. 101003598

method is of influence to the final results, as shown in Savelberg et al. (in review). Spatial patterns could completely shift between two methods, which is why it is important to always think about your target audience and the type of vulnerability (for/of whom/what) you want to assess.

Previous research has shown that it is possible to create a (social) vulnerability index on European scale. Here, we discuss two examples and the methods that they used. Reimann et al. (2024) produced a global social vulnerability index (GlobE-SoVI) via an inductive approach. They built a regression model with a stepwise approach in which different combinations of indicators were iteratively tested to find the best model fit. The independent variable are flood fatalities. The indicators that were in the best model fit were selected for the GlobE-SoVI. This is a simple sum of each indicator times their weight. The weights were determined by the indicator's regression coefficients. They find that globally the most important drivers of vulnerability are education levels, the gender-income gap, and for Western Europe also the share of elderly. However, as they mention themselves, "we are not able to establish exact causality in our analysis. Therefore, these variables may be proxies for a variety of other characteristics such as the quality of infrastructure, early warning systems, or the strength of local institutions". It would therefore be interesting to repeat the method on a smaller geographical scale with the more detailed indicators from Stolte et al. (in prep.).

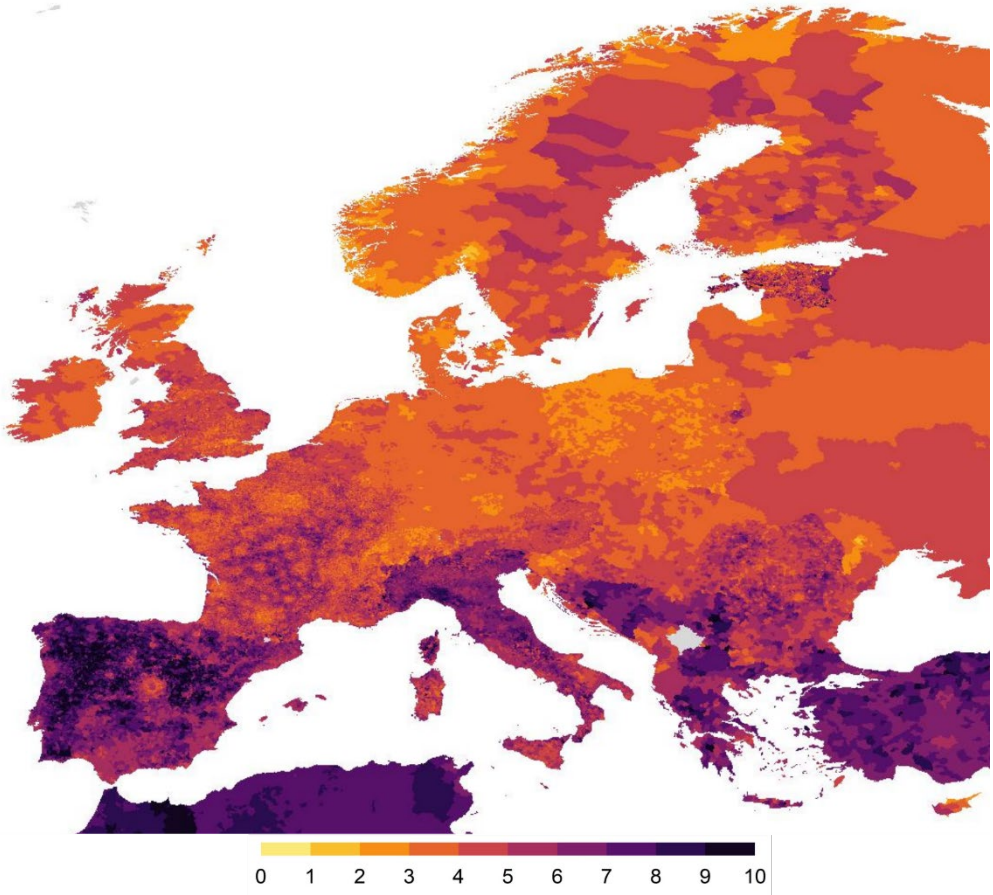

Figure 17. *Vulnerability index based on the work of Reimann et al. (2024). Figure adopted from Reimann et al. (2024)*

Tapia et al. (2017) perform an urban vulnerability analysis on 571 European cities. They apply another inductive approach, but this time the selection of indicators is done via PCA instead

This project has received funding from the European Union's Horizon 2020 research and innovation programme under grant agreement No. 101003598

of the regression technique from Reimann et al. (2024). Contrary to GlobE-SoVI, Tapia et al. (2017) develop the model for specific hazards, among which coastal floods. They emphasize that their results need to be interpreted as relative vulnerability and that there is no benchmark to compare the absolute vulnerability to. The results show that cities at the Atlantic coast, western Mediterranean and the Baltic are relatively more vulnerable than on the Italian Peninsula, the UK and Scandinavia. They attribute this partially to the difference in adaptive capacity (among others operationalized with the level of city committed to fight against climate change) and level of awareness (among others operationalised with Google search counts on coastal floods). Most of their data comes from Eurostat and is more specific than that from Reimann et al. (2024).

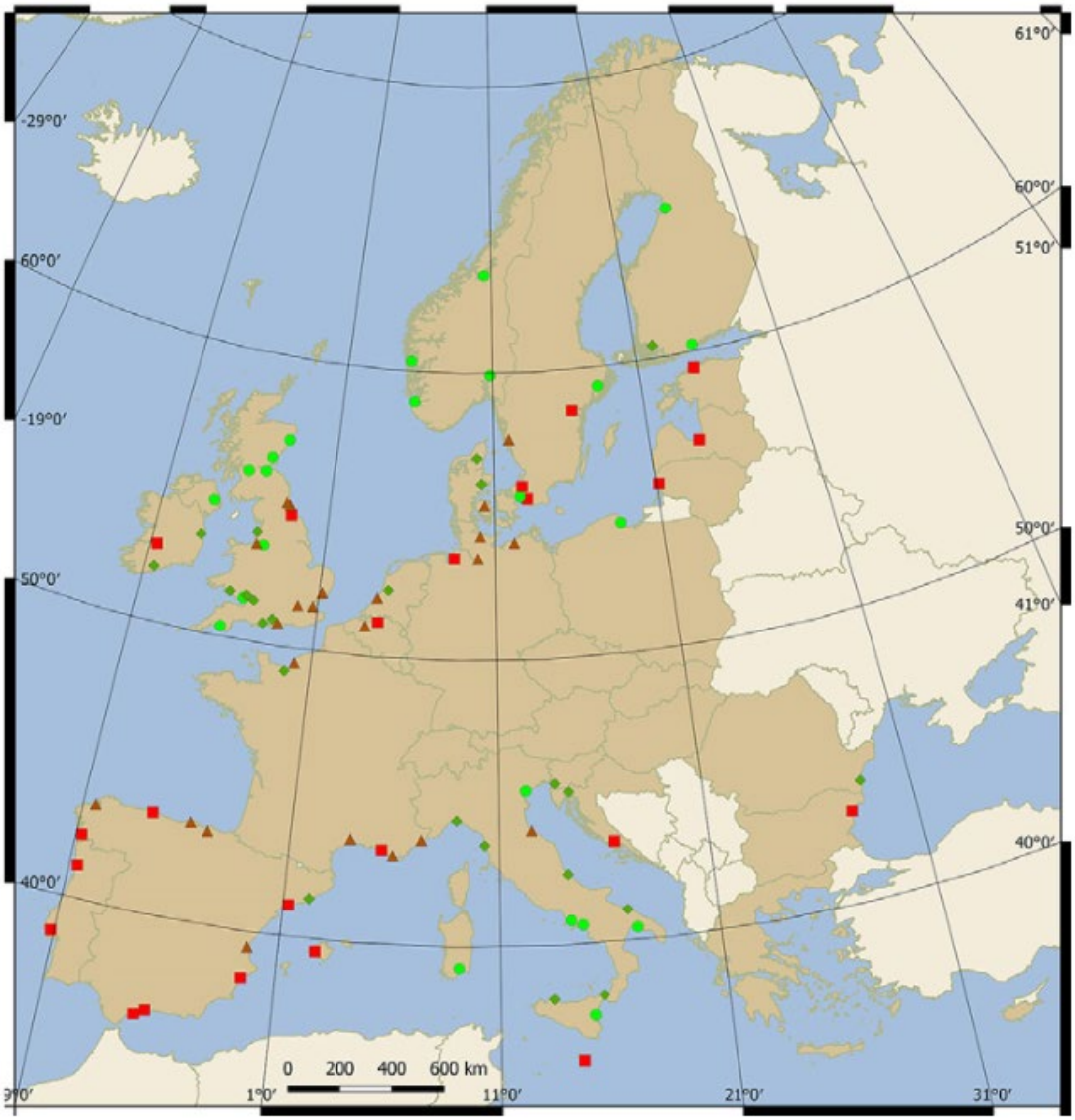

Figure 18. Vulnerability index for European coastal cities, based on the work of Tapia et al. (2017). Red squares = higher vulnerability (> quantile 0.75); Red triangles = medium to higher vulnerability (Median to quantile 0.75); Green diamonds = medium to lower vulnerability (quantile 0.25 to Median); Green circles = lower vulnerability (< quantile 0.25) Figure adopted from Tapia et al. (2017).

This project has received funding from the European Union's Horizon 2020 research and innovation programme under grant agreement No. 101003598

4. Discussion

First of all, it is important to note that vulnerability is a latent variable: a non-directly-observable inherent characteristic of a person or object. It can therefore never be explicitly assessed in its entirety, but instead it needs to be estimated indirectly using above-mentioned methods (Spielman et al., 2020). As a result, the choices that are made surrounding the input data and methods can strongly influence the results (Spielman et al., 2020; Tapia et al., 2017), which emphasises the importance of understanding the context in a vulnerability assessment (Spielman et al., 2020; Rufat et al., 2015; Hinkel, 2011). Both vulnerability curves as well as indicators/indexes therefore show only a part of the overall vulnerability, whilst simplifying it in the process (Tapia et al., 2017; Abson et al., 2012; Rufat, 2013).

Ideally, one would include different types of vulnerability dynamics in their assessments (de Ruiter & van Loon, 2022). Most vulnerability assessments are a snapshot in time, not accounting for temporal dynamics or evolving vulnerability, whereas – especially in cities – vulnerability is a highly volatile phenomenon. This mostly has to do with data limitations, as it is difficult to find comparable timeseries of data across cities. Nonetheless, several data variables in our overview allow for a temporally dynamic vulnerability assessment. Management (Eriksen et al., 2021; Schipper, 2020) and directional dynamics (Stolte et al., 2024) are other forms of vulnerability dynamics, which describe the non-linear or non-monotonic relationship between a vulnerability driver and the impact of a hazard. For instance, retired elderly that live inside a well-cooled home are probably less vulnerable to heat than young people working outside in the scorching sun (bi-direction vulnerability; Stolte et al., 2024), yet elderly are usually dubbed the most vulnerable population to heatwaves (Bambrick et al., 2011; Bradford et al., 2015; Huang et al., 2022). New methods have to be developed to also take into account these type of dynamics, for instance by combining indicators like age and retirement policy and validating them against heatwave impact data.

This project has received funding from the European Union's Horizon 2020 research and innovation programme under grant agreement No. 101003598

5. Conclusion

In Deliverable 5.3 of the CoCliCo project, we presented a detailed analysis of vulnerability assessments methods for coastal flooding, focusing on the impact of coastal flooding on European coastal communities, and the physical vulnerability of critical infrastructure systems in particular. To do so, we integrated academic and grey literature to develop a thorough understanding of flood vulnerability. Through a structured review, we identified and defined drivers of vulnerability to coastal flooding. Furthermore, we compiled a harmonized database containing 110 fragility and vulnerability curves for a wide range of infrastructure and building assets, facilitating well-informed decision-making in risk assessments. Moreover, based on the available data, we were able to operationalized 206 drivers of coastal flood vulnerability (out of 360 identified) for European coastal vulnerability assessments, aggregated into 34 quantifiable vulnerability indicators.

The main conclusions drawn from Deliverable 5.3 underscore the significant strides made in enhancing the understanding of vulnerability of coastal communities in the face of flooding. By collating a wealth of data and literature, the report provides valuable insights into the complex interplay of factors shaping vulnerability. However, we also acknowledge the inherent limitations of vulnerability assessments, emphasizing the need for caution in interpreting results and understanding the context in which they are derived. Despite these challenges, the deliverable serves as a useful resource for policymakers, researchers, and practitioners engaged in coastal climate risk assessments across Europe.

Looking ahead, the insights gained from this deliverable lay the groundwork for future research and policy interventions aimed at bolstering coastal community resilience. The harmonized database of fragility and vulnerability curves, coupled with the identification of coastal flood vulnerability drivers, provides a solid foundation for further exploration and refinement of coastal adaptation strategies. Moving forward, efforts should focus on addressing data gaps, refining methodologies, and integrating local-scale knowledge to enhance the applicability and robustness of vulnerability assessments. By leveraging these insights, stakeholders can better anticipate and mitigate the impacts of coastal flooding and sea-level rise on critical infrastructure and coastal communities in general, ultimately fostering a more resilient and sustainable future for European coastal societies.

This project has received funding from the European Union's Horizon 2020 research and innovation programme under grant agreement No. 101003598

References

Abson, D.J., Dougill, A.J., Stringer, L.C., 2012. Using Principal Component Analysis for information-rich socio-ecological vulnerability mapping in Southern Africa. Applied Geography 35, 515–524. https://doi.org/10.1016/j.apgeog.2012.08.004

Allen, T.R., Crawford, T., Montz, B., Whitehead, J., Lovelace, S., Hanks, A.D., Christensen, A.R., Kearney, G.D., 2019. Linking Water Infrastructure, Public Health, and Sea Level Rise: Integrated Assessment of Flood Resilience in Coastal Cities. Public works management & policy 24, 110–139. https://doi.org/10.1177/1087724X18798380

Araya-Muñoz, D., Metzger, M.J., Stuart, N., Wilson, A.M.W., Carvajal, D., 2017. A spatial fuzzy logic approach to urban multi-hazard impact assessment in Concepción, Chile. Science of The Total Environment 576, 508–519. https://doi.org/10.1016/j.scitotenv.2016.10.077

Bahlo, C., Dahlhaus, P., 2021. Livestock data – Is it there and is it FAIR? A systematic review of livestock farming datasets in Australia. Computers and Electronics in Agriculture 188, 106365. https://doi.org/10.1016/j.compag.2021.106365

Bambrick, H.J., Capon, A.G., Barniett, G.B., Beaty, R.M., Burton, A.J., 2011. Climate Change and Health in the Urban Environment: Adaptation Opportunities in Australian Cities. Asia-pacific journal of public health 23, 67S-79S. https://doi.org/10.1177/1010539510391774

Batica, J., Gourbesville, P., Erlich, M., Coulet, C., Mejean, A., 2018. Xynthia flood, learning from the past events - Introducing a FRI to stakeholders, in: Gourbesville, P., Cunge, J., Caignaert, G. (Eds.), Advances in Hydroinformatics. SimHydro 2017 - Choosing the Right Model in Applied Hydraulics. Springer Water, pp. 607–619.

Becker, A.H., Matson, P., Fischer, M., Mastrandrea, M.D., 2015. Towards seaport resilience for climate change adaptation: Stakeholder perceptions of hurricane impacts in Gulfport (MS) and Providence (RI). Progress in Planning, Towards seaport resilience for climate change adaptation: Stakeholder perceptions of hurricane impacts in Gulfport (MS) and Providence (RI) 99, 1–49. https://doi.org/10.1016/j.progress.2013.11.002

Bradford, K., Abrahams, L., Hegglin, M., Klima, K., 2015. A Heat Vulnerability Index and Adaptation Solutions for Pittsburgh, Pennsylvania. Environmental science & technology 49, 11303–11311. https://doi.org/10.1021/acs.est.5b03127

Bubeck, P., Dillenardt, L., Alfieri, L., Feyen, L., Thieken, A.H., Kellermann, P., 2019. Global warming to increase flood risk on European railways. Climatic Change 155, 19–36. https://doi.org/10.1007/s10584-019-02434-5

Bukvic, A., Gohlke, J., Borate, A., Suggs, J., 2018. Aging in Flood-Prone Coastal Areas: Discerning the Health and Well-Being Risk for Older Residents. International journal of environmental research and public health 15. https://doi.org/10.3390/ijerph15122900

Buontempo, C., Hanlon, H.M., Bruno Soares, M., Christel, I., Soubeyroux, J.-M., Viel, C., Calmanti, S., Bosi, L., Falloon, P., Palin, E.J., Vanvyve, E., Torralba, V., Gonzalez-Reviriego, N., Doblas-Reyes, F., Pope, E.C.D., Newton, P., Liggins, F., 2018. What have we learnt from EUPORIAS climate service prototypes? Climate Services 9, 21–32. https://doi.org/10.1016/j.cliser.2017.06.003

This project has received funding from the European Union's Horizon 2020 research and innovation programme under grant agreement No. 101003598

Cardona, O.D., Ordaz, M.G., Reinoso, E., Yamín, L.E., Barbat, A.H., 2012. CAPRA - Comprehensive Approach to Probabilistic Risk Assessment: International Initiative for Risk Management Effectiveness. Presented at the 15th World Conference on Earthquake Engineering, Lisbon, Portugal.

Chandra, A., Gaganis, P., 2016. Deconstructing vulnerability and adaptation in a coastal river basin ecosystem: a participatory analysis of flood risk in Nadi, Fiji Islands. Climate and development 8, 256–269. https://doi.org/10.1080/17565529.2015.1016884

Christodoulou, A., Christidis, P., Demirel, H., 2019. Sea-level rise in ports: a wider focus on impacts. Marit Econ Logist 21, 482–496. https://doi.org/10.1057/s41278-018-0114-z

Dal Cin, F., Hooimeijer, F., Matos Silva, M., 2021. Planning the Urban Waterfront Transformation, from Infrastructures to Public Space Design in a Sea-Level Rise Scenario: The European Union Prize for Contemporary Architecture Case. Water 13. https://doi.org/10.3390/w13020218

de Bruijn, K., Wagenaar, D., Slager, K., de Bel, M., Burzel, A., 2015. Updated and improved method for flood damage assessment: SSM2015 (version 2) (No. 1220043– 003). Deltares.

de Koning, K., Filatova, T., Need, A., Bin, O., 2019. Avoiding or mitigating flooding: Bottom-up drivers of urban resilience to climate change in the USA. Global environmental change-human and policy dimensions 59. https://doi.org/10.1016/j.gloenvcha.2019.101981

De Moel, H., Jongman, B., Kreibich, H., Merz, B., Penning-Rowsell, E., Ward, P.J., 2015. Flood risk assessments at different spatial scales. Mitig Adapt Strateg Glob Change 20, 865–890. https://doi.org/10.1007/s11027-015-9654-z

De Ruiter, M.C., Van Loon, A.F., 2022. The challenges of dynamic vulnerability and how to assess it. iScience 25, 104720. https://doi.org/10.1016/j.isci.2022.104720

De Ruiter, M.C., Ward, P.J., Daniell, J.E., Aerts, J.C.J.H., 2017. Review Article: A comparison of flood and earthquake vulnerability assessment indicators. Nat. Hazards Earth Syst. Sci. 17, 1231–1251. https://doi.org/10.5194/nhess-17-1231-2017

Djordjeviç, S., 2014. Project final report Collaborative research on flood resilience in urban areas.

Dottori, F., Kalas, M., Salamon, P., Bianchi, A., Alfieri, L., Feyen, L., 2017. An operational procedure for rapid flood risk assessment in Europe. Nat. Hazards Earth Syst. Sci. 17, 1111–1126. https://doi.org/10.5194/nhess-17-1111-2017

Eakin, H., Parajuli, J., Yogya, Y., Hernandez, B., Manheim, M., 2021. Entry points for addressing justice and politics in urban flood adaptation decision making. Current opinion in environmental sustainability 51, 1–6. https://doi.org/10.1016/j.cosust.2021.01.001

Eriksen, S., Schipper, E.L.F., Scoville-Simonds, M., Vincent, K., Adam, H.N., Brooks, N., Harding, B., Khatri, D., Lenaerts, L., Liverman, D., Mills-Novoa, M., Mosberg, M., Movik, S., Muok, B., Nightingale, A., Ojha, H., Sygna, L., Taylor, M., Vogel, C., West, J.J., 2021. Adaptation interventions and their effect on vulnerability in developing countries: Help, hindrance or irrelevance? World Development 141, 105383. https://doi.org/10.1016/j.worlddev.2020.105383

European Commission. Joint Research Centre., 2016. Global flood depth-damage functions: methodology and the database with guidelines. Publications Office, LU.

This project has received funding from the European Union's Horizon 2020 research and innovation programme under grant agreement No. 101003598

Fang, Z., Wu, Y., Zhong, H., Liang, J., Song, X., 2021. Revealing the impact of storm surge on taxi operations: Evidence from taxi and typhoon trajectory data. Environment and planning b-urban analytics and city science 48, 1463–1477. https://doi.org/10.1177/2399808320954206

Fekete, A., 2019. Social Vulnerability (Re-)Assessment in Context to Natural Hazards: Review of the Usefulness of the Spatial Indicator Approach and Investigations of Validation Demands. Int J Disaster Risk Sci 10, 220–232. https://doi.org/10.1007/s13753-019-0213-1

Findlater, K., Webber, S., Kandlikar, M., Donner, S., 2021. Climate services promise better decisions but mainly focus on better data. Nat. Clim. Chang. 11, 731–737. https://doi.org/10.1038/s41558-021-01125-3

Forzieri, G., Bianchi, A., Silva, F.B. e, Marin Herrera, M.A., Leblois, A., Lavalle, C., Aerts, J.C.J.H., Feyen, L., 2018. Escalating impacts of climate extremes on critical infrastructures in Europe. Global Environmental Change 48, 97–107. https://doi.org/10.1016/j.gloenvcha.2017.11.007

Frick-Trzebitzky, F., 2017. Crafting Adaptive Capacity: Institutional Bricolage in Adaptation to Urban Flooding in Greater Accra. Water alternatives-an interdisciplinary journal on water politics and development 10, 625–647.

Gandini, A., Garmendia, L., Prieto, I., Alvarez, I., San-Jose, J.-T., 2020. A holistic and multi-stakeholder methodology for vulnerability assessment of cities to flooding and extreme precipitation events. Sustainable cities and society 63. https://doi.org/10.1016/j.scs.2020.102437

Gargiulo, C., Battarra, R., Tremiterra, M.R., 2020. Coastal areas and climate change: A decision support tool for implementing adaptation measures. Land use policy 91. https://doi.org/10.1016/j.landusepol.2019.104413

Gerlak, A.K., Greene, C., 2019. Interrogating vulnerability in the Global Framework for Climate Services. Climatic Change 157, 99–114. https://doi.org/10.1007/s10584-019-02384-y

Huang, Y., Yang, J., Chen, J., Shi, H., Lu, X., 2022. Association between ambient temperature and age-specific mortality from the elderly: Epidemiological evidence from the Chinese prefecture with most serious aging. Environmental research 211. https://doi.org/10.1016/j.envres.2022.113103

Hultquist, C., Simpson, M., Cervone, G., Huang, Q., 2015. Using nightlight remote sensing imagery and Twitter data to study power outages, in: Proceedings of the 1st ACM SIGSPATIAL International Workshop on the Use of GIS in Emergency Management. Presented at the SIGSPATIAL'15: 23rd SIGSPATIAL International Conference on Advances in Geographic Information Systems, ACM, Bellevue Washington, pp. 1–6. https://doi.org/10.1145/2835596.2835601

Increasing infrastructure resilience background report, 2019. . Miyamoto International, World Bank, Washington, D.C.

Irish, J.L., Frey, A.E., Rosati, J.D., Olivera, F., Dunkin, L.M., Kaihatu, J.M., Ferreira, C.M., Edge, B.L., 2010. Potential implications of global warming and barrier island degradation on future hurricane inundation, property damages, and population impacted. Ocean & coastal management 53, 645–657. https://doi.org/10.1016/j.ocecoaman.2010.08.001

Jeuken, A., Haasnoot, M., Reeder, T., Ward, P., 2015. Lessons learnt from adaptation planning in four deltas and coastal cities. Journal of water and climate change 6, 711–728. https://doi.org/10.2166/wcc.2014.141

This project has received funding from the European Union's Horizon 2020 research and innovation programme under grant agreement No. 101003598

Joakim, E.P., Mortsch, L., Oulahen, G., Harford, D., Klein, Y., Damude, K., Tang, K., 2016. Using system dynamics to model social vulnerability and resilience to coastal hazards.

Jongman, B., Kreibich, H., Apel, H., Barredo, J.I., Bates, P.D., Feyen, L., Gericke, A., Neal, J., Aerts, J.C.J.H., Ward, P.J., 2012. Comparative flood damage model assessment: towards a European approach. Nat. Hazards Earth Syst. Sci. 12, 3733–3752. https://doi.org/10.5194/nhess-12-3733-2012

Jonkman, S.N., Hillen, M.M., Nicholls, R.J., Kanning, W., van Ledden, M., 2013. Costs of Adapting Coastal Defences to Sea-Level Rise-New Estimates and Their Implications. Journal of coastal research 29, 1212–1226. https://doi.org/10.2112/JCOASTRES-D-12-00230.1

Kellermann, P., Schöbel, A., Kundela, G., Thieken, A.H., 2015. Estimating flood damage to railway infrastructure – the case study of the March River flood in 2006 at the Austrian Northern Railway. Natural Hazards and Earth System Sciences 15, 2485–2496. https://doi.org/10.5194/nhess-15-2485-2015

Kellermann, P., Schönberger, C., Thieken, A.H., 2016. Large-scale application of the flood damage model RAilway Infrastructure Loss (RAIL). Natural Hazards and Earth System Sciences 16, 2357–2371. https://doi.org/10.5194/nhess-16-2357-2016

Kok, M., Huizinga, H.J., Vrouwenvelder, A.C.W.M., Barendregt, A., 2005. Standard Method Damage and casualties caused by flooding.pdf (No. DWW-2005-009). Road and Hydraulic Engineering Institute, Rijkswaterstaat.

Koks, E.E., Le Bars, D., Essenfelder, A.H., Nirandjan, S., Sayers, P., 2023. The impacts of coastal flooding and sea level rise on critical infrastructure: a novel storyline approach. Sustainable and Resilient Infrastructure 8, 237–261. https://doi.org/10.1080/23789689.2022.2142741

Koks, E.E., van Ginkel, K.C.H., van Marle, M.J.E., Lemnitzer, A., 2022. Brief communication: Critical infrastructure impacts of the 2021 mid-July western European flood event. Natural Hazards and Earth System Sciences 22, 3831–3838. https://doi.org/10.5194/nhess-22-3831-2022

Kreibich, H., Piroth, K., Seifert, I., Maiwald, H., Kunert, U., Schwarz, J., Merz, B., Thieken, A.H., 2009. Is flow velocity a significant parameter in flood damage modelling? Nat. Hazards Earth Syst. Sci. 9, 1679–1692. https://doi.org/10.5194/nhess-9-1679-2009

Kuhlicke, C., Madruga De Brito, M., Bartkowski, B., Botzen, W., Doğulu, C., Han, S., Hudson, P., Nuray Karanci, A., Klassert, C.J., Otto, D., Scolobig, A., Moreno Soares, T., Rufat, S., 2023. Spinning in circles? A systematic review on the role of theory in social vulnerability, resilience and adaptation research. Global Environmental Change 80, 102672. https://doi.org/10.1016/j.gloenvcha.2023.102672

Lasage, R., Veldkamp, T.I.E., de Moel, H., Van, T.C., Phi, H.L., Vellinga, P., Aerts, J.C.J.H., 2014. Assessment of the effectiveness of flood adaptation strategies for HCMC. Natural hazards and earth system sciences 14, 1441–1457. https://doi.org/10.5194/nhess-14-1441-2014

Lindersson, S., Brandimarte, L., Mård, J., Di Baldassarre, G., 2020. A review of freely accessible global datasets for the study of floods, droughts and their interactions with human societies. WIREs Water 7, e1424. https://doi.org/10.1002/wat2.1424

McKenna, G., Argyroudis, S.A., Winter, M.G., Mitoulis, S.A., 2021. Multiple hazard fragility analysis for granular highway embankments: Moisture ingress and scour. Transportation Geotechnics 26, 100431. https://doi.org/10.1016/j.trgeo.2020.100431

This project has received funding from the European Union's Horizon 2020 research and innovation programme under grant agreement No. 101003598

Meijer, L.G., Reimann, L., Aerts, J.C.J.H., 2023. Comparing spatially explicit approaches to assess social vulnerability dynamics to flooding. International Journal of Disaster Risk Reduction 96, 103883. https://doi.org/10.1016/j.ijdrr.2023.103883

Meltzer, R., Ellen, I.G., Li, X., 2021. Localized commercial effects from natural disasters: The case of Hurricane Sandy and New York City. Regional science and urban economics 86. https://doi.org/10.1016/j.regsciurbeco.2020.103608

Menoni, S., Molinari, D., Parker, D., Ballio, F., Tapsell, S., 2012. Assessing multifaceted vulnerability and resilience in order to design risk-mitigation strategies. Nat Hazards 64, 2057–2082. https://doi.org/10.1007/s11069-012-0134-4

Meyer, V., Becker, N., Markantonis, V., Schwarze, R., Van Den Bergh, J.C.J.M., Bouwer, L.M., Bubeck, P., Ciavola, P., Genovese, E., Green, C., Hallegatte, S., Kreibich, H., Lequeux, Q., Logar, I., Papyrakis, E., Pfurtscheller, C., Poussin, J., Przyluski, V., Thieken, A.H., Viavattene, C., 2013. Review article: Assessing the costs of natural hazards – state of the art and knowledge gaps. Nat. Hazards Earth Syst. Sci. 13, 1351–1373. https://doi.org/10.5194/nhess-13-1351-2013

Meyer, V., Messner, F., 2005. National flood damage evaluation methods. A review of applied methods in England, the Netherlands, the Czech Republic and Germany.

Montoya-Rincon, J.P., Azad, S., Pokhrel, R., Ghandehari, M., Jensen, M.P., Gonzalez, J.E., 2022. On the Use of Satellite Nightlights for Power Outages Prediction. IEEE Access 10, 16729–16739. https://doi.org/10.1109/ACCESS.2022.3149485

Multi-hazard Loss Estimation Methodology. Flood model. (Technical manual), n.d. . Federal Emergency Management Agency (FEMA), Washington, D.C.

Mycoo, M.A., 2014. Autonomous household responses and urban governance capacity building for climate change adaptation: Georgetown, Guyana. Urban climate 9, 134–154. https://doi.org/10.1016/j.uclim.2014.07.009

Nirandjan, S., Koks, E.E., Ye, M., Pant, R., van Ginkel, K.C.H., Aerts, J.C.J.H., Ward, P.J., 2024. Review article: Physical Vulnerability Database for Critical Infrastructure Multi-Hazard Risk Assessments – A systematic review and data collection. Natural Hazards and Earth System Sciences Discussions 1–38. https://doi.org/10.5194/nhess-2023-208

OIEWG, 2016. Report of the open-ended intergovernmental expert working group on indicators and terminology relating to disaster risk reduction (No. A/71/644). United Nations.

Papathoma-Köhle, M., 2016. Vulnerability curves vs. vulnerability indicators: application of an indicator-based methodology for debris-flow hazards. Nat. Hazards Earth Syst. Sci. 16, 1771–1790. https://doi.org/10.5194/nhess-16-1771-2016

Pinto, P.J., Kondolf, G.M., Wong, P.L.R., 2018. Adapting to sea level rise: Emerging governance issues in the San Francisco Bay Region. Environmental science & policy 90, 28–37. https://doi.org/10.1016/j.envsci.2018.09.015

Qu, K., Yao, W., Tang, H.S., Agrawal, A., Shields, G., Chien, S.I., Gurung, S., Imam, Y., Chiodi, I., 2021. Extreme storm surges and waves and vulnerability of coastal bridges in New York City metropolitan region: an assessment based on Hurricane Sandy. Natural hazards 105, 2697–2734. https://doi.org/10.1007/s11069-020-04420-y

Ramos, F.R., Uitermark, J., 2021. An introduction to DUIA: The database on urban inequality and amenities. PLoS ONE 16, e0253824. https://doi.org/10.1371/journal.pone.0253824

This project has received funding from the European Union's Horizon 2020 research and innovation programme under grant agreement No. 101003598

Reimann, L., Koks, E., De Moel, H., Ton, M.J., Aerts, J.C.J.H., 2024. An Empirical Social Vulnerability Map for Flood Risk Assessment at Global Scale ("GlobE-SoVI"). Earth's Future 12, e2023EF003895. https://doi.org/10.1029/2023EF003895

Robin, E., Acuto, M., 2018. Global urban policy and the geopolitics of urban data. Political Geography 66, 76–87. https://doi.org/10.1016/j.polgeo.2018.08.013

Rodriguez, R., 2001. Internationale Kommission zum Schutz des Rheines (IKSR).

Rufat, S., 2013. Spectroscopy of Urban Vulnerability. Annals of the Association of American Geographers 103, 505–525. https://doi.org/10.1080/00045608.2012.702485

Schipper, E.L.F., 2020. Maladaptation: When Adaptation to Climate Change Goes Very Wrong. One Earth 3, 409–414. https://doi.org/10.1016/j.oneear.2020.09.014

Sendai Framework for Disaster Risk Reduction 2015 - 2030, 2015. . United Nations Office for Disaster Risk Reduction, Geneva, Switzerland.

Spielman, S.E., Tuccillo, J., Folch, D.C., Schweikert, A., Davies, R., Wood, N., Tate, E., 2020. Evaluating social vulnerability indicators: criteria and their application to the Social Vulnerability Index. Nat Hazards 100, 417–436. https://doi.org/10.1007/s11069-019-03820-z

Spiteri, D., Gauci, R., 2022. Coastal Flood Risks and the Business Community: Stakeholders' Perception in Malta. Climate 10. https://doi.org/10.3390/cli10090132

Stolte, T.R., Koks, E.E., de Moel, H., Reimann, L., van Vliet, J., de Ruiter, M.C., Ward, P.J., 2024. VulneraCity–drivers and dynamics of urban vulnerability based on a global systematic literature review. International Journal of Disaster Risk Reduction 108, 104535. https://doi.org/10.1016/j.ijdrr.2024.104535

Stolte, T.R., Koks, E.E., De Moel, H., Reimann, L., van Vliet, J., De Ruiter, M.C., Ward, P.J., 2023. VulneraCity - The urban vulnerability drivers database. https://doi.org/10.5281/zenodo.8282815

Stolte, T.R., Koks, E.E., De Moel, H., Reimann, L., van Vliet, J., de Ruiter, M.C., Ward, P.J., in review. VulneraCity - drivers and dynamics of urban vulnerability based on a global systematic literature review.

Tapia, C., Abajo, B., Feliu, E., Mendizabal, M., Martinez, J.A., Fernández, J.G., Laburu, T., Lejarazu, A., 2017. Profiling urban vulnerabilities to climate change: An indicator-based vulnerability assessment for European cities. Ecological Indicators 78, 142–155. https://doi.org/10.1016/j.ecolind.2017.02.040

Tate, E., 2012. Social vulnerability indices: a comparative assessment using uncertainty and sensitivity analysis. Nat Hazards 63, 325–347. https://doi.org/10.1007/s11069-012-0152-2

Tiggeloven, T., De Moel, H., Winsemius, H.C., Eilander, D., Erkens, G., Gebremedhin, E., Diaz Loaiza, A., Kuzma, S., Luo, T., Iceland, C., Bouwman, A., Van Huijstee, J., Ligtvoet, W., Ward, P.J., 2020. Global-scale benefit–cost analysis of coastal flood adaptation to different flood risk drivers using structural measures. Nat. Hazards Earth Syst. Sci. 20, 1025–1044. https://doi.org/10.5194/nhess-20-1025-2020

Tsubaki, R., Bricker, J.D., Ichii, K., Kawahara, Y., 2016. Development of fragility curves for railway embankment and ballast scour due to overtopping flood flow. Nat. Hazards Earth Syst. Sci. 16, 2455–2472. https://doi.org/10.5194/nhess-16-2455-2016

This project has received funding from the European Union's Horizon 2020 research and innovation programme under grant agreement No. 101003598

Van Ginkel, K.C.H., Dottori, F., Alfieri, L., Feyen, L., Koks, E.E., 2021. Flood risk assessment of the European road network. Nat. Hazards Earth Syst. Sci. 21, 1011–1027. https://doi.org/10.5194/nhess-21-1011-2021

van Zelst, V.T.M., Dijkstra, J.T., van Wesenbeeck, B.K., Eilander, D., Morris, E.P., Winsemius, H.C., Ward, P.J., de Vries, M.B., 2021. Cutting the costs of coastal protection by integrating vegetation in flood defences. Nature communications 12. https://doi.org/10.1038/s41467-021-26887-4

Vanneuville, W., Maddens, R., Collard, C., Bogaert, P., De Maeyer, P., Antrop, M., n.d. Impact op mens en economie t.g.v. overstromingen bekeken in het licht van wijzigende hydraulische condities, omgevingsfactoren en klimatologische omstandigheden. België, Vlaanderen.

Vousdoukas, M.I., Mentaschi, L., Hinkel, J., Ward, P.J., Mongelli, I., Ciscar, J.-C., Feyen, L., 2020. Economic motivation for raising coastal flood defenses in Europe. Nat Commun 11, 2119. https://doi.org/10.1038/s41467-020-15665-3

Vousdoukas, M.I., Voukouvalas, E., Annunziato, A., Giardino, A., Feyen, L., 2016. Projections of extreme storm surge levels along Europe. Clim Dyn 47, 3171–3190. https://doi.org/10.1007/s00382-016-3019-5

Wannewitz, M., Garschagen, M., 2021. Review article: Mapping the adaptation solution space - lessons from Jakarta. Natural hazards and earth system sciences 21, 3285–3322. https://doi.org/10.5194/nhess-21-3285-2021

Ward, P.J., De Ruiter, M.C., Mård, J., Schröter, K., Van Loon, A., Veldkamp, T., Von Uexkull, N., Wanders, N., AghaKouchak, A., Arnbjerg-Nielsen, K., Capewell, L., Carmen Llasat, M., Day, R., Dewals, B., Di Baldassarre, G., Huning, L.S., Kreibich, H., Mazzoleni, M., Savelli, E., Teutschbein, C., Van Den Berg, H., Van Der Heijden, A., Vincken, J.M.R., Waterloo, M.J., Wens, M., 2020. The need to integrate flood and drought disaster risk reduction strategies. Water Security 11, 100070. https://doi.org/10.1016/j.wasec.2020.100070

Wilson, M.T., 2020. Assessing voluntary resilience standards and impacts of flood risk information. Building research and information 48, 84–100. https://doi.org/10.1080/09613218.2019.1642731

Yepes-Estrada, C., Silva, V., Rossetto, T., D'Ayala, D., Ioannou, I., Meslem, A., Crowley, H., 2016. The Global Earthquake Model Physical Vulnerability Database. Earthquake Spectra 32, 2567–2585. https://doi.org/10.1193/011816EQS015DP

Yoon, D.K., 2012. Assessment of social vulnerability to natural disasters: a comparative study. Nat Hazards 63, 823–843. https://doi.org/10.1007/s11069-012-0189-2

Zarghami, S.A., Dumrak, J., 2021. A system dynamics model for social vulnerability to natural disasters: Disaster risk assessment of an Australian city. International Journal of Disaster Risk Reduction 60, 102258. https://doi.org/10.1016/j.ijdrr.2021.102258

This project has received funding from the European Union's Horizon 2020 research and innovation programme under grant agreement No. 101003598